ABSTRACT

TIME DEPENDENT STRENGTH BEHAVIOR OF TWO
SOIL TYPES AT LOWERED TEMPERATURES

by Ilham AlNouri

This study is concerned with the time-dependent deformation behavior of two frozen soils, under a specified stress-history and a range of temperatures, and the feasibility of developing time-dependent strength parameters for frozen soils. Part of the behavior study was to observe the creep deformation in the steady state region, and to determine the effect of temperature, stress difference, mean normal stress, and soil type on the creep rate of frozen soil.

Two soil types were used; Sault Ste. Marie clay and standard Ottawa sand. The cylindrical samples were one square inch in cross section and 2.26 inches high. The clay was premixed to the desired water content and compressed to the desired density, then trimmed to the specified sample size, while the sand samples were cast in an aluminum mold. The samples were tested in a triaxial cell submerged in low-temperature bath, with the temperature controlled to within ± 0.05 degrees Centigrade. Two types of test were conducted on both soil types. The first type

was a differential creep test in which the axial stress difference was maintained constant and the confining pressure was increased in increments. The differential creep tests were conducted at several values of constant axial loading on duplicate samples, and at several test temperatures. The creep deformations were recorded continuously during the test. The second type of test conducted was a constant axial strain-rate test performed on duplicate samples of frozen Sault Ste. Marie clay and frozen saturated sand at relatively fast strain-rates and at -12° C.

The results of the differential creep tests on frozen Sault Ste. Marie clay and frozen saturated sand indicate that the creep rate of frozen soil at a constant test temperature increases exponentially with increase in axial stress difference, and decreases exponentially with the increase in mean stress. This indicates that the mean stress does affect the creep rate of frozen soil. According to the results of the differential creep tests, two equations describing the steady state creep deformation were developed; the first determines the effect of stress on creep rate of frozen soil at constant temperature, and the second equation determines the effect of temperature on creep rate under constant stress difference. A third equation has been suggested, to estimate the creep rate of frozen soil under the effect of both temperature and stress.

To provide more information on the time-dependent strength behavior of frozen soil, differential creep test results were used to develop time-dependent strength parameter; a cohesion C, and an angle of friction ϕ. For a specific creep rate, we can determine the values of major and minor principal stress σ_1 and σ_3, for each test, and then use these values to sketch a modified Mohr plot which shows the values of C and ϕ that correspond to that specific creep rate. The cohesion C decreases with a slower creep rate, implying the dependence of C on time, while the friction angle ϕ appears to remain constant with change in creep rate.

The constant axial strain-rate tests were used to determine the strength parameters of frozen soils at a relatively high strain-rate, and to determine the effect of confining pressure on the ultimate strength of the two soil types. The confining pressure has no significant effect on the ultimate strength of frozen clay, while the ultimate strength of frozen saturated sand does increase with increase in confining pressure, therefore implying the development of friction during deformation of frozen saturated sand.

TIME DEPENDENT STRENGTH BEHAVIOR OF TWO SOIL TYPES AT LOWERED TEMPERATURES

By

Ilham AlNouri

A THESIS

Submitted to
Michigan State University
in partial fulfillment of the requirements
for the degree of

DOCTOR OF PHILOSOPHY

Department of Civil Engineering

January 1969

925782
6-6-69

ACKNOWLEDGMENTS

The writer is deeply indebted to his major professor, Dr. O. B. Andersland, Professor of Civil Engineering, for his continuous encouragement and assistance, and greatly appreciates the time he devoted most generously to discussions and consultations. The writer also wishes to express his gratitude to Dr. L. E. Malvern, Professor of Applied Mechanics, for his many helpful comments and suggestions. Thanks are also due the other members of the writer's doctoral committee: Dr. C. E. Cutts, Chairman and Professor of Civil Engineering; Dr. R. K. Wen, Professor of Civil Engineering, and Dr. D. W. Hall, Professor of Mathematics. The writer wishes to express his appreciation to Dr. R. R. Goughnour, Associate Professor of Civil Engineering, for his assistance and consultations concerning the testing equipment.

Thanks are also due the National Science Foundation and the Division of Engineering Research at Michigan State University for the financial assistance that made this study possible.

TABLE OF CONTENTS

LIST OF FIGURES

Figure		Page

LIST OF TABLES

NOTATIONS

C = cohesion

D = $\sigma_1 - \sigma_3$ = axial stress difference

f = shear force acting on a flow unit

ΔF = free energy of activation, cal. per mole

h = Plank's constant = 6.624×10^{-7} erg-sec^{-1}

k = Boltzmann's constant = 1.38×10^{-16} erg °K^{-1}

ℓ, m, n = creep parameters

$p = \frac{\sigma_1 + \sigma_3}{2}$

$q = \frac{\sigma_1 - \sigma_3}{2}$

R = universal gas constant = 1.98 cal°K^{-1} mole^{-1}

T = temperature in degrees Centigrade or absolute temperature

t = time

γ = frequency of activation, sec^{-1}

X = parameter relating activation frequency to strain rate

ϕ = angle of internal friction

λ = distance between equilibrium positions of flow units

γ_d = dry density

w = water content, percent

ε = true axial strain

$\dot{\varepsilon} = \frac{d\varepsilon}{dt}$ = true axial strain-rate, or creep rate in the steady state creep region

σ_1 = major principal stress

σ_3 = minor principal stress, or confining pressure

$\sigma_D = \sigma_1 - \sigma_m$ = deviatoric stress

$\sigma_m = \frac{1}{3}(\sigma_1 + \sigma_2 + \sigma_3)$ = hydrostatic stress or mean normal stress

$\Sigma = D - \sigma_m$

$\bar{\varepsilon}$ = equivalent strain or intensity of shear strain

$\bar{\sigma}$ = equivalent stress or intensity of shear stress

CHAPTER I

INTRODUCTION

Soils in general are considered as a three phase material; solid particles, water, and gas. With decrease in temperature below freezing, the water will partially or almost completely change to ice, with the unfrozen water content dependent on the temperature and certain soil properties. Now the soil becomes a complex four phase system, in which the four components are interrelated. The phase change of water is accompanied by an increase in adhesion between the soil particles, liquid water, and ice together with drastic changes in the physical and mechanical properties of the soil.

Shear strength of frozen soil depends on several factors including soil type, homogeneity, water content including ice content, temperature, mode of freezing, normal stress, and deformation rates. The most significant factor determining the strength properties of a frozen soil is the temperature below freezing. The ultimate compressive strength increases drastically with decrease in temperature.

Frozen soils, in general, exhibit a high value of instantaneous resistance to deformation. However, tests show that if the load is applied for a long time, the resistance of frozen soils to external forces decreases considerably. The influence of time of load on the strength of frozen soils is evident by comparing them with unfrozen soils; the strength of frozen soils is lowered with time to a much greater degree. Thawed soils, for all practical purposes, display no loss of strength with time. Nevertheless, frozen soils under the continuous action of a load have a strength several times greater than that of unfrozen soils of the same type.

Frozen and unfrozen soils commonly fail by shear under the influence of concentrated loads. The shear strength of unfrozen soil can be described, using the Mohr-Coulomb failure theory, by two parameters: an angle of internal friction ϕ and cohesion C. However, tests show that the shear strength of frozen soils is time-dependent. Thus, the need arises to develop time-dependent strength parameters. One phase of this study is concerned with the study of such parameters for two soil types, a cohesive soil (Sault Ste. Marie clay) and a cohesionless soil (Ottawa sand).

The second phase of this study is concerned with an effort to describe and determine the deformation behavior of these soils for a specified stress history and range of temperature. In general, frozen soil behavior is approximated by an elasto-plasto-viscous body, since all the deformations inherent in such bodies may develop, depending upon the stress and its time factor. Since design problems are concerned with a long term behavior, one must consider the range of stresses that cause undamped creep. Thus, design problems are concerned mainly with a plasto-viscous type behavior (steady state creep). The presence of ice and unfrozen water constitute the viscous element in the material and are responsible for the development of rheological processes.

Existing creep theories do not take the influence of the mean stress on deformation behavior into consideration (Vialov, 1965a). Since the equivalent strain $\bar{\varepsilon}$, in frozen and unfrozen soils, is not only a function of the equivalent stress $\bar{\sigma}$, but also of the mean stress σ_m, the effect of the mean stress on the creep rate of the frozen soil has been included in this study in an effort to provide more information on the time-dependent behavior of frozen soil. Differential triaxial creep tests were planned and conducted on frozen saturated Sault Ste. Marie clay and frozen saturated Ottawa sand. For a given test, the axial loading was maintained constant and the confining pressure was increased in increments, implying that in a triaxial type apparatus, the deviatoric stress is held constant while the mean stress is increased or decreased by increments. The creep rate was observed at several stress levels, under different axial loadings. The effect of temperature on deformation rates was observed by conducting differential creep tests at several test temperatures under similar stress conditions. To minimize the effect of soil properties such as density, water content, and soil type, the tests were conducted on duplicate samples of both soil types. The experimental results indicate that creep rates and time-dependent strength parameters can be predicted with a reasonable degree of accuracy once certain soil parameters have been evaluated.

CHAPTER II

LITERATURE REVIEW

1. Frozen Soil Structure

"Frozen Soil" is a term applied to those soils in which below freezing temperatures exist and in which at least a part of the water contained in the soil pores is frozen. The ice matrix formed serves to cement the soil particles into a much more coherent mass (Tsytovich, 1960). Frozen soil is a complex four phase system consisting of four interrelated component materials: solid mineral particles and ice, liquid water, and air or gas.

The physico-mechanical processes present in freezing soils produce properties and structure of frozen soils which are quite different from those of unfrozen soils. A partial or almost complete change of water into ice, which occurs in freezing soils, is accompanied by the appearance of new ice cementation bonds between the mineral particles of the soil, and by sharp changes in the physical and mechanical properties of the soil. During the further cooling of frozen soils, especially in zones of intensive phase changes of water in the frozen soils, there occurs continuously the redistribution of moisture and the movement of water toward the line of cooling and freezing, and the subsequent freezing of water drawn up to the frost line.

Change in the temperature of frozen soil changes the phase composition of water in frozen soil, which in turn controls the degree of cementation of particles by ice. However, at any temperature below freezing there always remain a certain amount of unfrozen water (Tsytovich, 1960). Since the cementation bond in frozen soil is a function of the ice content, it is necessary to determine the amount of unfrozen water at any temperature, which can be estimated with a reasonable accuracy, on the basis of certain measurable soil properties (Dillon and Andersland, 1966).

2. Strength of Frozen Soils

Under the influence of concentrated loads both frozen and thawed soils commonly fail by shear. According to the Mohr-Coulomb failure theory, the shear strength S along any place is a function of normal stress σ on that plane, or

$$S = C + \sigma \tan \phi \qquad (2\text{-}1)$$

wherein C is the intercept on the shearing stress axis and ϕ is the angle of internal friction. The quantities C and ϕ are material properties which are dependent on soil temperature, soil type, soil density, and time of loading. For cohesionless soils the failure envelope normally passes through the origin (C = 0). When moist or saturated soil is exposed to freezing temperatures, the free water contained in the voids freezes, whereupon the ice interconnects the soil particles and the shear strength increases at zero normal stress (increase in C value).

The cohesion in thawed soils is some function of the molecular attraction between solid particles, which may be separated by water films, the amount of such particle separation, and the specific area of the soil particles. These forces increase with reduction in particle spacing (greater density). In frozen soils, the mineral particles and ice grains are generally separated by a thin film of unfrozen water, and the forces between soil particles and ice are greatly increased with reduction in temperature. Some Russian scientists consider this increased cohesion analogous to "cementation." Cohesion in frozen soils is not constant (Vialov, 1965b), but varies with change in ice content and time; it also depends on the structural changes in the ice contained in the soil. Polycrystalline ice will deform with time under very small stresses (Dillon and Andersland, 1967). This type of cohesion, in frozen soils, is the least stable part of cohesion, since it changes with any variation of the temperature field.

For a given pressure and temperature, a state of thermodynamic equilibrium exists between the ice and unfrozen water in frozen soil (Vialov, 1965b). A load applied to the soil disturbs the equilibrium condition, and may cause partial melting of ice. Under the influence of an increasing stress gradient, the water film may be displaced from a region of greater stress to one of smaller stress, where it again freezes. Plastic flow of the ice occurs at the same time. The flow of ice and the moisture shift is usually accompanied by: breaking up of the structural bonds, displacement of solid particles, and reorientation of the ice crystals. As this process continues, it leads to the growth of creep deformation and to the reduction of the strength of the soil as well. At the same time, the processes cause regrouping of the particles, recrystallization of the ice, and re-establishment of bonds.

The instantaneous resistance of frozen soils is generally large. However, under the continued effect of a constant load, frozen soils yield under pressures which are many times smaller. This peculiarity of frozen soils is governed mainly by the plastic properties of ice contained in the soil voids and the molecular bonds between ice and the mineral particles.

Constant stress-rate tests conducted by Tsytovich (1960) on different types of frozen soils showed that ultimate strength is proportional to the decrease in temperature, and that the frozen sands were characterized by a much higher value of ultimate compressive strength as compared to that of frozen clay. However, the resistance of frozen soils to external forces decreased considerably when the loads were applied for a long time, due to the relaxation of the ice-cementation cohesion. Frozen soils fail under much smaller loads when the loading is of long duration.

The strength of any material is described by its shear strength. Shear strength of frozen soils is a function of at least three variables:

$$\tau = f\ (T,\ P,\ t)\ . \qquad (2\text{-}2)$$

where T is the temperature of soil below freezing, P is normal pressure, and τ is the time of action of the load. Tsytovich (1960) considered frozen soils as analogous to over-consolidated soils, therefore assuming a proportionality between shear strength and normal pressure in the form:

$$\tau = C_T + P \tan \phi_T\ . \qquad (2\text{-}3)$$

where C_T is cohesion, ϕ_T is the angle of internal friction at temperature T. At a temperature of 0°C, the angle of internal friction ϕ is practically equal to the angle of internal friction of unfrozen soil, but the cohesion of frozen soil is much higher (see Figure 2-1). As an approximation, this made it possible to neglect the internal friction in evaluating the shear strength of frozen soils. Tsytovich (1960) suggested a ball penetration test for effective determination of the cohesive force.

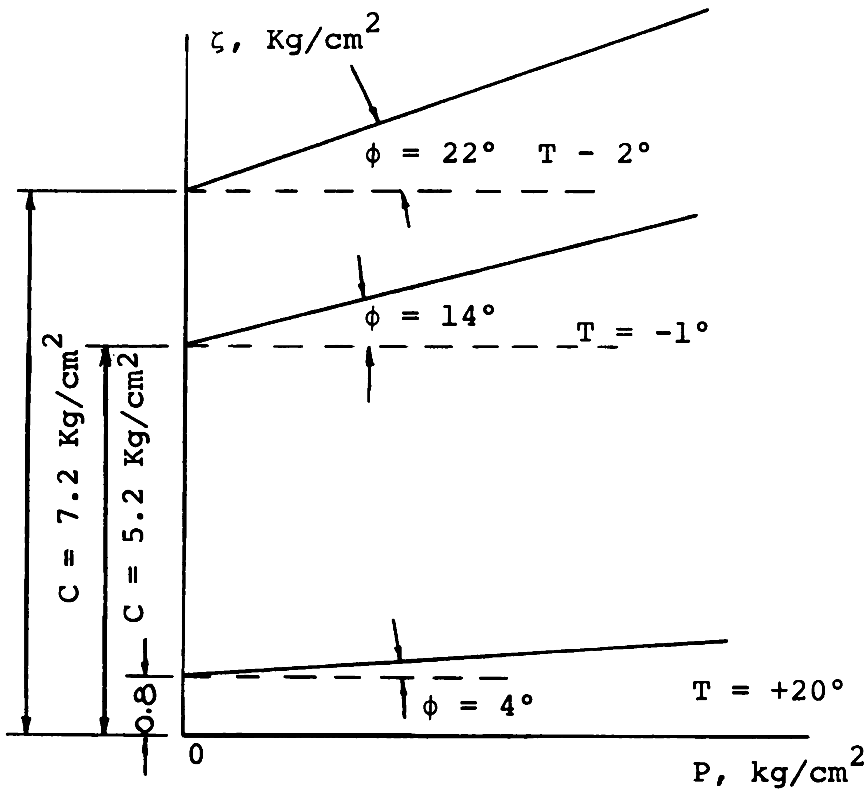

Figure 2-1. Relation Between Shear Strength of Frozen Soil and Temperature. (After Tsytovich, 1960).

Constant strain-rate tests conducted on frozen sand-ice samples (Goughnour and Andersland, 1968), showed that the ultimate shear strength of sand-ice material increased with the increase in strain-rate and with the decrease in temperature, and that the ultimate strength increased sharply with the increase in the volume concentration of sand in the sand-ice samples. For a sand concentration above 42%, it appears that particles contact is established. The relation between Peak strength and strain-rate, temperature, and sand volume concentration is shown in Figure 2-2.

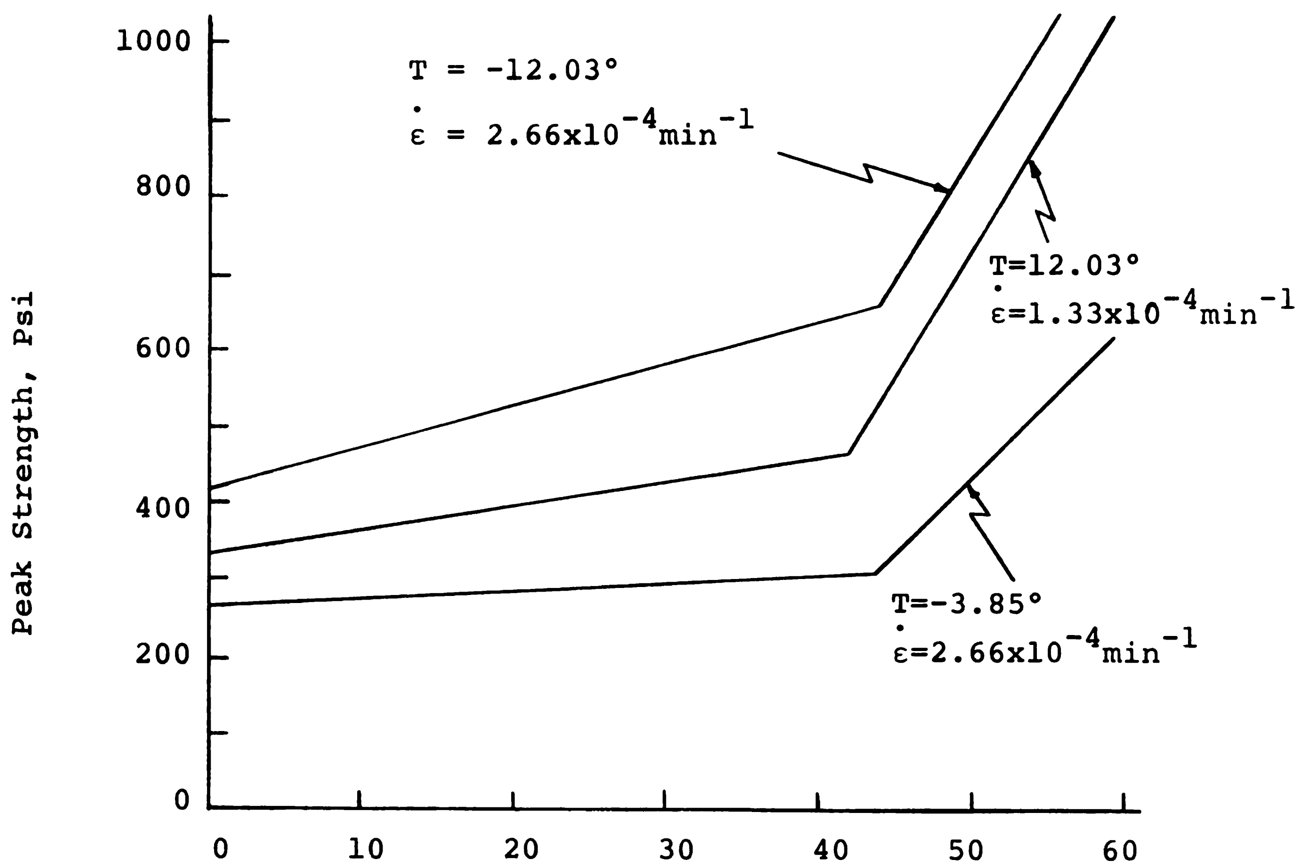

Figure 2-2. Peak Strength Versus Percent Sand By Volume. (After Goughnour, 1967).

3. Rheological Properties of Frozen Soils

Creep is defined as the time-dependent deformation of materials which occurs under constant stress and temperature. Frozen soils exhibit such a behavior, a deformation increase with time, under a constant uniaxial stress (Vialov, 1965a). Figure 2-3a shows typical creep curves, which represent the relationship between strain ε, and time t. Each curve corresponds to a given constant axial stress σ. The magnitude of stress determines the nature of the creep curve. If the stress does not exceed a certain limit, which is usually defined as a limiting long-term strength, then the deformation is damped (damped creep); if the stress does exceed the above mentioned limit, then undamped creep develops, leading eventually to failure.

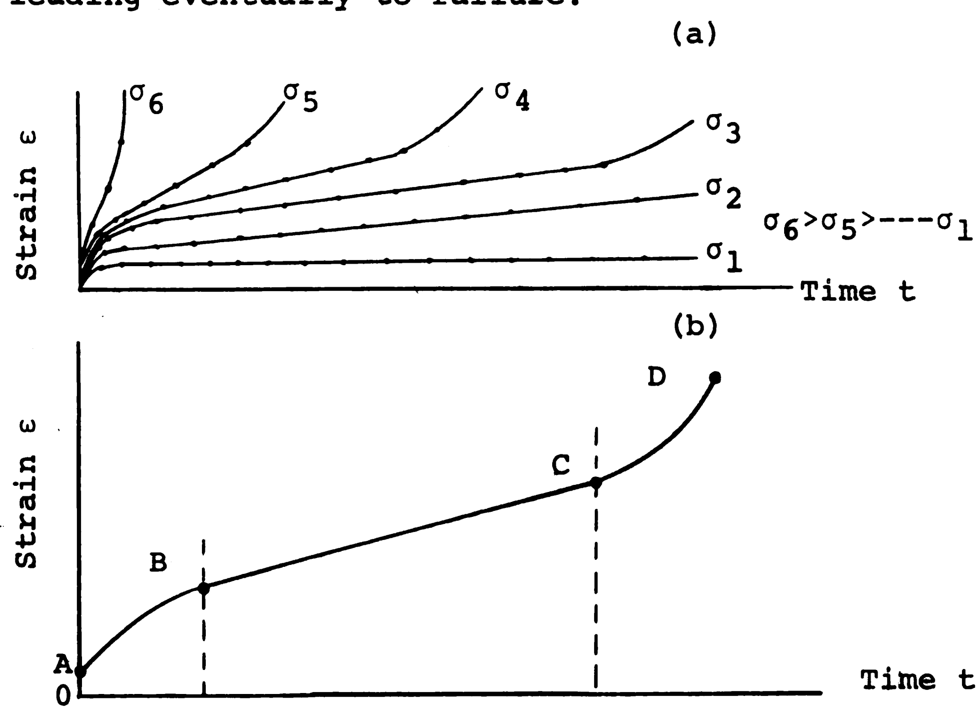

Figure 203a. Creep Curves for Frozen Soils. (After Vialov, 1965a).

In general, creep curves for frozen soils correspond to classical creep curves, and could be divided into four stages (see Figure 2-3b).

1. Instantaneous Strain: represents the strain which occurs upon application of the load. This deformation may be either elastic or elasto-plastic, depending upon the value of such load. Upon removal of the load, this deformation will be completely recovered in the elastic case, and partially recovered in the elasto-plastic case. This deformation is represented by section O-A of the creep curve.

2. Primary or Transient Creep: represents the stage of deformation which grows at a decreasing rate. For a damped deformation process, the rate of deformation will continuously decrease until it approaches zero. For undamped deformation, the creep rate will continue to decrease until it reaches a minimum value (depending upon the value of stress). This stage is represented by A-B section of the creep curve.

3. Secondary or Steady-State Creep: represents the region of relatively constant creep rate. This stage is represented by B-C section of the creep curve.

4. Tertiary Creep: represents the final stage of the creep curve, in which the deformation grows at an increasing rate (progressive flow), and leading eventually to failure. This stage is represented by C-D section of the creep curve.

It is evident that the creep curve in itself does not identify the detailed mechanisms which operate during the deformation. However, this identity of creep curves indicates that they all undergo a similar sequence of rate-determining changes. During creep one can consider that two types of processes operate (Conrad, 1961): One increases resistance to flow (strain harding), the other decreases the resistance (recovery). If hardening predominates, the creep rate continually decreases (primary creep); a balance between hardening and recovery yields a constant creep rate (steady-state creep). Tertiary creep occurs if recovery is faster than hardening.

It is now generally accepted that creep is a thermally activated process. From a physical standpoint, this seems to be the most reasonable explanation for the increase in strain with time under the conditions of constant stress and temperature. It has been shown, for frozen soils, that a plot of the logarithm of creep rate versus the reciprocal of temperature yields a straight line, in accord with theories of thermally activated processes (Andersland and Akili, 1967). With this background, rate process theory must be considered in formulating any expression for prediction of frozen soil behavior.

4. Rate Process Theory and Frozen Soil Behavior

The rate process theory (Glasstone, Laidler, and Eyring, 1941) can be applied to any process involving the time-dependent rearrangement of matter, so it could be used to describe and predict soil behavior such as creep or consolidation (Mitchell, Campanella, and Singh, 1968).

The basis of the theory is that the atoms and molecules participating in a deformation process (termed flow units) are constrained from movement relative to each other by energy barriers separating adjacent equilibrium positions. This is shown schematically by curve A in Figure 2-4.

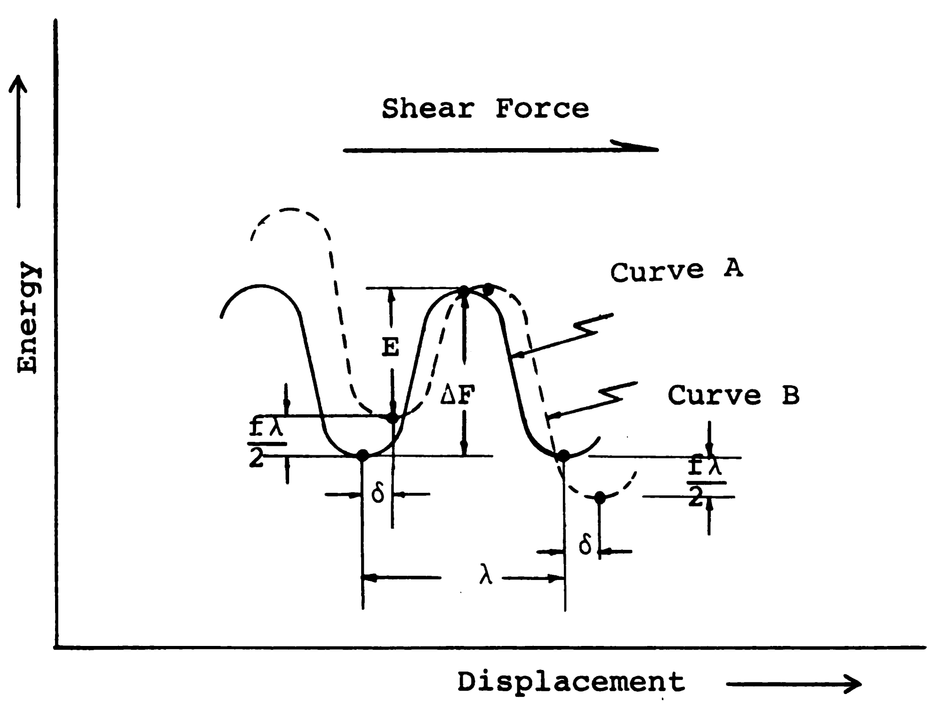

Figure 2-4. Representation of Energy Barrier Separating Equilibrium Positions.

The displacement of flow units to new positions requires that they become activated through aquisition of sufficient activation energy, ΔF, to overcome the energy barrier. From statistical mechanics, it is known that the flow units are continuously vibrating with a frequency of kT/h, as a consequence of their thermal energy, where
k = Boltzman's constant (1.38×10^{-16} erg - $°K^{-1}$),
h = Planck's constant (6.624×10^{-2} erg - sec^{-1}), and
T = the absolute temperature, °K. The division of thermal energies among the flow units is given by a Boltzmann distribution, and the specific frequency of activation, ν, may be shown to be

$$\nu = \frac{kT}{h} e^{-\Delta F/RT} \tag{2-4}$$

in which R = Universal Gas Constant = 1.98 cal° K^{-1} mol^{-1}.

If a shear stress is applied to the material, the barrier heights become distorted. This is shown by curve B in Figure 2-4. The distance, λ, represents the distance between successive equilibrium positions. If f represents the force acting on a flow unit, then the barrier height is reduced by $f\lambda/2$ in the direction of the force and raised by the same amount in the opposite direction. The elastic distortion of the material causes the minimums of the energy curve to be displaced a distance, δ.

Since the barrier height becomes $(\Delta F - f\lambda/2)$ in the direction of the force, and $(\Delta F + f\lambda/2)$ in the opposite direction, the net frequency of activation in the direction of the force becomes

$$\vec{\nu} - \overleftarrow{\nu} = 2\,\frac{kT}{h}\exp\left(\frac{-\Delta F}{RT}\right)\sinh\left(\frac{f\lambda}{2kT}\right) \qquad (2\text{-}5)$$

If a parameter, X, is defined which is a function of the number of flow units and the average component of displacement in the direction of deformation, then the total displacement per unit time will be:

$$\dot{\varepsilon} = X\,(\vec{\nu} - \overleftarrow{\nu}) \qquad (2\text{-}6)$$

$$\dot{\varepsilon} = 2X\,\frac{kT}{h}\exp\left(\frac{-\Delta F}{RT}\right)\sinh\left(\frac{f\lambda}{2kT}\right) \qquad (2\text{-}7)$$

If creep in frozen soils is thermally activated, as experimental data have indicated (Andersland and Akili, 1967), one can write for the creep rate $\dot{\varepsilon}$

$$\dot{\varepsilon} \propto \exp\left(\frac{-\Delta F}{RT}\right) \qquad (2\text{-}8)$$

Rate process theory supports a general creep equation (Conrad, 1961) of the form

$$\dot{\varepsilon} = \sum_i C_i\,(\sigma,T,S)\exp\left[\frac{-\Delta F_i(\sigma,T,S)}{RT}\right]\sinh\,[B_i(T,S)\sigma] \qquad (2\text{-}9)$$

where C_i is the frequency factor and B_i is the stress factor. C_i, ΔF_i, and B_i may correspond to one of i number of deformation mechanisms. The frequency factor and activation energy may depend on stress σ, temperature T, and frozen soil structure S. The stress factor may depend on temperature and structure. Although a number of deformation mechanisms may be operating simultaneously, usually one is rate controlling so that an evaluation of equation (2-9) is possible by gross mechanical measurements (Conrad, 1961). For one deformation mechanism controlling, and stress conditions such that sinh $B\sigma \simeq 1/2$ exp $B\sigma$, equation (2-9) may be written

$$\dot{\varepsilon} = C \exp\left(\frac{-\Delta F}{RT}\right) \exp\ (B\sigma) \qquad (2\text{-}10)$$

If temperature is held constant, the effect of stress on the creep rate could be developed, while at constant stress, the effect of temperature could be developed.

CHAPTER III

SOILS STUDIED AND SAMPLE PREPARATION

Two soil types were used in this study. The first, a cohesive soil, was a red glacial clay obtained from the vicinity of Sault Ste. Marie, Michigan. This clay will be referred to as Sault Ste. Marie clay. The second soil used was a cohesionless material, a standard Ottawa Sand.

The properties of the two soils and the procedures for sample preparation are described below:

1. Frozen Clay Sample

The Sault Ste. Marie clay has been used in previous studies conducted at Michigan State University. It is pedologically classified as Ontonagon. A summary of the index properties of this clay, and the results of mineralogical test on it, are listed in Table 3-1 below.

To minimize the effect of differences in density, water content, and degree of saturation between test specimens, duplicate samples were prepared. This was achieved by mixing a precalculated weight of air dried Sault Ste. Marie clay (Passing 1/4 in. Sieve) with a

Table 3-1.--Physical and Mineralogical Properties of Sault Ste. Marie Clay

Liquid Limit	60%
Plastic Limit	24%
Plasticity Index	36%
Specific Gravity	2.78
Gradation (% finer by weight)	
2 mm.	100%
0.06 mm.	90%
0.002 mm.	60%
<u>For Material Less Than 2μ:</u>	
1. Specific Surface Area	290 m^2/gram
2. Cation Exchange Capacity	28 meg/100 gram
3. Mineral Content:	
Illite	50%
Vermiculite	20%
Chlorite	15%
Kaolinite	5%
Quartz and Feldspar	10%

calculated weight of distilled water and compressing the mixture to a specified volume having the desired density, water content, and degree of saturation. Distilled, deaerated, and deionized water was used in preparing the clay samples.

The calculations were based on the following design values: (1) a dry density of 100 pounds per cubic foot, and (2) a degree of saturation of 96%. After mixing the calculated weights of air dried clay and distilled water, the mixture was left for three days in an airtight container to insure uniform distribution of moisture in the clay. Afterwards, the mixture was placed in an 11 inch diameter split mold and compacted statically to the predetermined height of 4 inches. The procedure of compaction was previously developed by Leonards (1955). The compaction produced a cake 11 inches in diameter and 4 inches high, and resulted in a dry density of 102.5 pounds per cubic foot and a water content of 24.5%. The cake was then cut into prismatic samples 2 × 2 inches in cross section and 4 inches high. Each sample was immediately wrapped with a polyethelyene sheet, covered with aluminum foil, and coated with several coats of wax. Then, the samples were numbered and stored under water.

Prior to testing, the wax was removed and a water content sample was taken, then the specimen was trimmed in a soil lathe to a cylindrical shape approximately 1.13 inches in diameter (one square inch in cross sectional area). The top and bottom of the sample were trimmed in an aluminum mold to give a height of approximately 2.26 inches. After recording the diameter, height, and weight of the sample, lucite discs were placed on each end of the sample with friction reducer discs in between. The friction reducers were made by coating both sides of a sheet of aluminum foil with a very thin layer of silicone grease. A thin polyethylene film was then applied to both sides of the aluminum foil. The excess grease and any entrapped air were worked out by a straight edge. The sheet was then cut into discs of the proper diameter. The clay sample was then mounted on top of the force transducer in the triaxial cell. Two rubber membranes were placed over the sample, and several rubber bands were tightly placed on both caps and the pedestal to prevent leakage and loss of moisture prior to and during testing. The top of the triaxial cell was placed in position and tightened. The cell was filled with the coolant, an equal portion mixture of ethylene glycol and water. Then the cell was carefully placed in a low-temperature bath, where the temperature was set about 3°C lower than the desired test temperature. The cell was left at that temperature for twenty-four hours so that the clay sample would freeze. At the end of the twenty-four hours, the temperature in the low-temperature bath was raised to the desired test temperature, and left for another twenty-four hours to insure temperature equilibrium prior to testing. Freezing at temperatures at least 3° below test temperature insured that ice contents of frozen samples correspond to the maximum possible in each test sample (Leonards and Andersland, 1960). The time allowed for freezing the clay sample and the duration allowed for the cold bath to reach and maintain a steady state test temperature were kept constant for all prepared samples, so that the effect of aging on the freezing process and the structure of the frozen clay would be minimized. The sample was then ready for testing.

After testing, the sample was weighed and left to dry in the oven, then weighed again. This was done to determine the sample's water content, and served as a check as to whether any leakage had occurred during the test. From checking density and water content for all the clay samples used, before and after testing, it was found that the maximum variation in water content between samples did not exceed 0.5%. And the variation in density was less than one pound per cubic foot.

2. Sand-Ice Samples

A standard Ottawa sand and distilled, deaerated, and deionized water were used to prepare all the sand-ice samples needed. The sand was sieved and only that portion which passed a number 20 sieve and retained on a number 30 sieve was used in preparing the samples. The specific gravity of the sand was 2.65.

All samples were cast in an aluminum split mold 1.13 inches in diameter, which gave an initial sample cross sectional area of one square inch. The height of the mold was 2.26 inches. A sand-ice sample was prepared by taking a predetermined weight of dry sand, so that it would give a 64% concentration, by volume, of sand particles in the sample. This particular percentage was chosen for convenience and to insure an interparticle contact between the sand particles (Goughnour and Andersland, 1968). The 64% sand volume concentration was used for all the sand-ice samples tested. A thin coat of silicone grease was applied to the interior of the mold to minimize adhesion between the frozen sample and the mold. The sand was poured into the mold, and the mold was tapped lightly on the side in order that the predetermined weight of sand would fill the volume of the mold, so that the top of the sand would be flush with the top of the mold. Precooled water was then poured into the mold to fill the pores between the sand particles. Great care was taken in doing that, so the compacted sand would not be disturbed. Then the mold was placed in a freezer at a temperature of -20°C and left to freeze for twenty-four hours. After freezing, the top of the sample was trimmed flush with the top of the mold. Prior to mounting the sample, the triaxial cell and the two plexiglass caps were cooled for three hours in the freezer. The mold was dismantled and the sand-ice sample was placed inside the triaxial cell with a plexiglass cap at both ends of the sample. A friction reducer was placed between the cap and the sample at both ends. Then two rubber membranes were placed on the sample and held at both ends with several rubber bands. Afterwards, the top of the triaxial cell was placed tightly in position and the cell was filled with precooled etheylene glycol and water mixture. The entire process of preparing the sand-ice sample and mounting it in the triaxial cell was done inside the freezer, in order to maintain the sand-ice system at low temperature and to prevent it from thawing. To change the sample temperature to the required test temperature, the triaxial cell was lowered into the low-temperature bath, which was previously set at the test temperature. The cell was left for twenty-four hours, so that the sample would reach the test temperature, and to insure temperature equilibrium. The time for freezing the sand-ice sample and the duration required for the sample to reach and maintain a steady state test temperature were kept constant for all prepared samples to minimize the effect of aging on the freezing process and the structure of the various sand-ice samples.

At the end of each test, the sand-ice sample was weighed, melted and dried in the oven, and the weight of the dry sand was recorded. From these measurements, the density of the sand-ice sample, the dry density of the sand sample, and the density of the ice matrix were calculated. The prepared sand-ice samples were based on the following design values:

Cross sectional area	=	1 sq. inch.
Height	=	2.26 inch.
Volume concentration of sand	=	64%
Dry density	=	107.5 Pcf.

For all the sand-ice samples prepared, the total density of the frozen saturated sand was (128 ± 0.5) Pcf. and the water content of the unfrozen samples was (19.4 ± 0.2) %. The bulk density of the ice matrix, based on the weight of the melted ice and the total volume of voids, was found to be (0.91 ± 0.005) gm/cm^3 at -12°C. The actual density of ice is a function of temperature (Pounder, 1967):

$$\gamma = 0.9168\ (1 - 1.53 \times 10^{-4}T) \qquad (3\text{-}1)$$

where γ is the density of ice in gm/cm^3 at temperature T, and T is in degrees Centigrade. Using equation (3-1), the density of ice at -12°C is 0.91848 gm/cm^3. This density was used to estimate the volume of air voids in the frozen saturated soil. The air voids in the prepared sand-ice samples were found to be less than 1% of the ice matrix.

CHAPTER IV

EQUIPMENT AND TEST PROCEDURES

1. Equipment

The same triaxial cell and cold bath were used for the differential creep tests and the constant axial strain-rate tests. The sample rested on a brass pedestal in a standard triaxial cell. The pedestal was mounted directly on a force transducer (DYNISCO Model TCFTS-1M), which has a rated capacity of 1000 pounds with overload to 1500 pounds. Figure 4-1 shows a schematic diagram of the sample placement in the triaxial cell. The triaxial cell was entirely submerged in a coolant, an equal part mixture of ethylene glycol and water. The coolant was maintained at a constant test temperature by circulating through a microregulator controlled cold box.

Before any testing was carried on, the temperature control was calibrated by measuring the temperature at the vicinity of the sample inside the triaxial cell, and the temperature at a fixed location in the low-temperature bath. The temperature of the sample was measured by placing a copper-constantan thermocouple adjacent to the sample at mid-height, and another one in a bath of distilled,

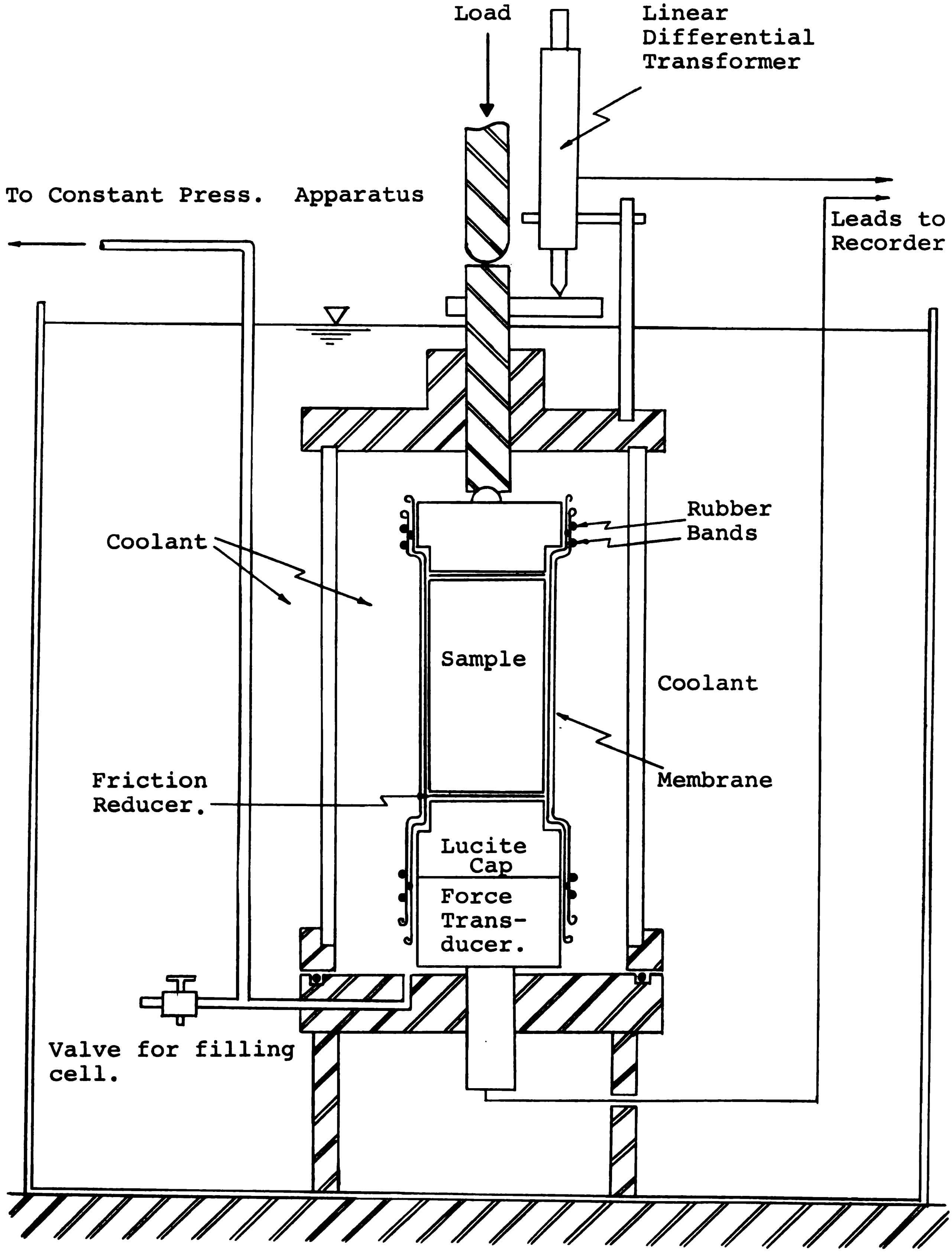

Figure 4-1. A Schematic Diagram of the Sample Placement in the Triaxial Cell.

deionized, melting ice used as a reference point. The temperature was obtained by measuring the E,M.F. with a potentiometer (Leeds and Northrop Model K-2) and using an E.M.F.-Temperature calibration chart. At the same time the temperature was measured at specific locations in the low-temperature bath by a thermometer with scale divisions of 0.1°C. These temperature measurements were carried on over a period of twenty-four hours. It was observed that the temperature varied by no more than 0.05°C. The bath temperature control was set at the desired test temperature and left for three days until the temperature at the bath reached a constant value of the desired test temperature. Prior to testing the sample was left for twenty-four hours in the low-temperature bath to insure temperature equilibrium in the sample.

The axial pressure was supplied through the loading ram at the top of the triaxial cell. The confining pressure was supplied through a valve at the base of the triaxial cell from a constant pressure unit. The pressure unit was a self-compensating mercury control apparatus, which was capable of supplying a constant pressure to a triaxial cell for testing over long periods. The pressure was provided through the valve assembly by the difference in head between the surface of mercury in the upper moving pots and the lower fixed pots. The constant pressure apparatus is shown in Figure 4-2.

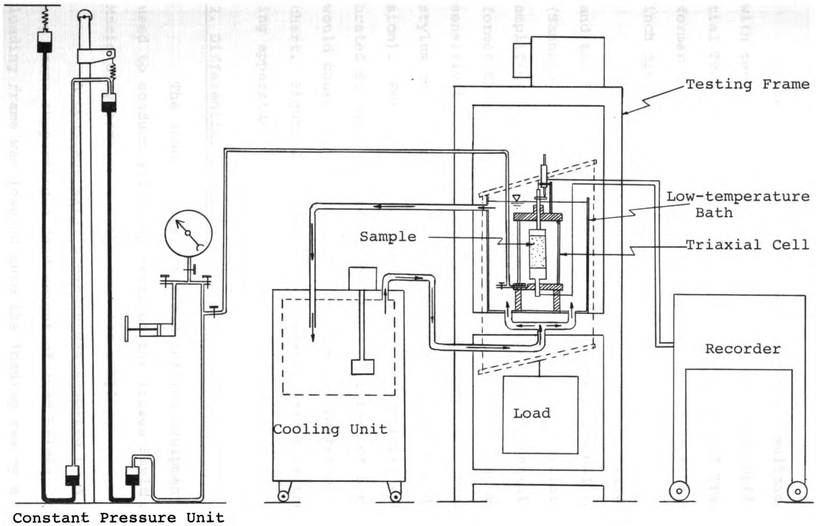

Figure 4-2. Diagramatic Layout of the Testing Apparatus.

The axial deformation was measured simultaneously with two different measuring devices, a Linear Differential Transformer (Sanborn Linearsyn Differential Transformer Model No. 575 DT-500), and a dial gauge with 0.0001 inch divisions.

The outputs of the linear differential transformer and the force transducer were fed into a 2-channel recorder (Sanborn Recorder Model 7702B with a Sanborn Carrier Preamplifier Model 8805A). For the linear differential transformer the preamplifier was calibrated so that, at maximum sensitivity, a deflection of 0.00025 inches will cause the stylus to deflect one millimeter on the chart (one division). For the force transducer the preamplifier was calibrated so that, at maximum sensitivity, a load of 5 pounds would cause the stylus to deflect one centimeter on the chart. Figure 4-2 shows a diagrammatic layout of the testing apparatus.

2. Differential Creep Tests

The same triaxial cell and testing equipment were used to conduct all creep tests on the frozen Sault Ste. Marie clay samples and the sand-ice samples.

A constant axial pressure was supplied by a loading frame supporting a dead weight of lead bricks. The loading frame was lowered onto the loading ram by a mechanical loading device at a relatively fast rate. It took less than 5 seconds for the total load to transfer to the sample through the ram. And since the dynamic effects are very small, they were assumed to be negligible. To compensate for the increase in cross sectional area as the sample deformed, lead shots were added to the dead load. The axial stress measured at the bottom of the sample and the axial deflection measured at the top of the sample were both recorded continuously on the charts of the recorder, at the highest possible sensitivity of the recording system. By observing the axial deflection data it was possible to know when the creep process had passed the primary creep stage and entered the steady state creep stage. When that stage was reached, and with axial loading constant, an increment of confining pressure was applied on the sample for a period of thirty minutes. Then the confining pressure was increased by four more increments of the same value, each increment applied for the same duration. In some of the creep tests, the confining pressure was decreased at the end of the test by increments of the same value, and the axial creep deformation was observed. The creep test was conducted with temperature held constant for at least twenty-four hours prior to testing, and all through the test period.

3. Constant Axial Strain-Rate Test

The same equipment and procedure were used for all constant axial strain-rate tests on the frozen Sault Ste. Marie clay and the sand-ice samples. Since the ultimate strengths of the frozen soil samples were expected to exceed the force transducer's loading capacity, a 5000 pound proving ring was used to measure the axial load. The load was applied directly to the loading ram by a variable speed mechanical loading system. A deformation rate of 0.00678 inch per minute was used. The deformation rate was maintained during the test, and periodically adjusted to give an approximate constant strain rate of 3×10^{-3} inch per inch per minute. Results showed that the variation was less than 10% when observed over two minute periods. The constant axial strain-rate tests were conducted with three different constant confining pressures of 30 Psi, 60 Psi, and 90 Psi. The confining pressure was applied prior to the axial loading in each case.

CHAPTER V

EXPERIMENTAL RESULTS

1. Differential Creep Tests

The creep tests were conducted to study the behavior of frozen soils under the effect of constant axial loading, and different values of confining pressures. The confining presure was increased by increments of 30 Psi, and maintained for 30 minutes for all creep tests, except Test No. C-4, in which the confining pressure increment was 20 Psi. By keeping the axial loading constant and increasing the confining pressure in the triaxial cell, the stress difference $D = (\sigma_1 - \sigma_3)$, and the deviatoric stress $\sigma_D = (\sigma_1 - \sigma_m)$, were kept constant, and the mean stress σ_m and the major principal stress σ_1 were increased by the same increment.

Typical creep tests on frozen Sault Ste. Marie clay samples, at a temperature of -12°C, with different values of axial loading, are shown in Figures 5-1a and 5-1b. These curves show the increase in true strain with respect to time under different confining pressures and a constant axial loading. Note that in the first portion of the curve, for which the confining pressure is zero, the shape of the curve conforms to the classical "Creep Curve". At the beginning, the strain increases at a high rate, then the creep rate starts to decrease progressively, implying strengthening, until it reaches a constant rate, which signifies the end of the primary creep region and the beginning of the steady state creep region. When the confining pressure was increased, there was a sharp rise in the strain ~ time curve, then the sample deformed at another constant creep rate (see Figure 5-2). The magnitude of the sudden rise in strain, when an additional confining pressure increment was applied to the sample, was approximately constant for all tests. Calculations show that this rise was caused by the expansion in the triaxial cell due to the increase in the confining pressure. For some of the creep tests, at the end of which the confining pressure was decreased by increments, a delayed response in deformation was observed upon the decrease in confining pressure, then the strain increased at a constant rate. This delayed response in strain with respect to time, at the beginning of the confining pressure decrement, could be due to a delayed response in the sample and the testing system. This behavior is shown in Figure 5-2.

It is evident from the creep curves in Figures 5-1a and 1b, that the steady state creep rate $\dot{\varepsilon}$ decreased, under a constant axial loading, with the increase in confining pressure. The creep rate for each loading condition was numerically evaluated from the true strain ~ time curve for every test. A summary of the differential creep tests on the Sault Ste. Marie clay, at a temperature of -12°C, with the stresses for each stage of the test and the corresponding steady state creep rates, are listed in Table 5-1. Experimental data are given in the Appendix.

Typical curves of the differential creep tests conducted on sand-ice samples, with a 64% volume concentration of sand and a test temperature of -12°C, are shown in Figures 5-3a and 5-3b for axial loads of 764.3 Psi and 815.9 Psi, respectively. The confining pressure increments were similar to those used for the clay samples. The shapes of the true strain ~ time curves of the sand-ice samples are similar to those of the frozen clay samples. The creep rate $\dot{\varepsilon}$ decreased, under a constant axial load, with the increase in confining pressure. A summary of the differential creep tests on the sand-ice samples, at a test temperature of -12°C, including the stresses for each stage of the test and the corresponding steady state creep rates, are listed in Table 5-2. Experimental data are given in the Appendix.

In creep Test No. S-4, conducted on a sand-ice sample at a temperature of -12°C, the axial creep rates were observed under an axial creep load of 764.3 Psi and confining pressure values of 0 and 30 Psi, next the axial creep load was increased to a value of 815.9 Psi, and the creep rates were observed for confining pressures of 30 Psi and 60 Psi. The true strain ~ time curve for creep Test No. S-4 is shown in Figure 5-4.

To determine the effect of temperature variations on the time-dependent behavior of frozen soils, differential creep tests were conducted at test temperatures of -10°C, -12°C, -14°C, and -18°C on duplicate sand-ice samples under a constant axial loading equal to 764.3 Psi. Figures 5-5a and 5-5b show true strain-time curves for creep tests at temperatures of -10°C and -18°C, respectively. By comparing these two curves with the one in Figure 5-3a, conducted on a duplicate sample under the same stress conditions and a test temperature of -12°C, a similar type of deformation behavior is observed. The magnitude of deformation varies with respect to the change in test temperature. This will be discussed in the next chapter. A summary of the differential creep tests conducted on duplicate sand-ice samples at different test temperatures, under the same axial loading, including the stresses at all stages of the test and the corresponding steady state creep rates, are listed in Table 5-3. Experimental data are given in the Appendix.

2. Constant Strain-Rate Tests

Constant axial strain-rate tests were used to determine the strength of the frozen soils at a relatively fast strain-rate of 3×10^{-3} in./in./min., with constant confining pressures of 30 Psi, 60 Psi, and 90 Psi. All tests were conducted at a constant test temperature of -12°C.

The stress-strain curves for constant axial strain-rate tests on identical Sault Ste. Marie clay samples are shown in Figures 5-6, 5-7, and 5-8. These figures also include the strain-time relation for each test. The stress-strain curve shape did not show a distinctive peak value. The stress increased rapidly with increase in strain, reaching an optimum value around 12% strain. The ultimate strength values were approximately the same for all tests conducted on duplicate Sault Ste. Marie clay samples subjected to different confining pressures. This indicates that confining pressure has little or no effect on the ultimate strength of the frozen clay samples at a high degree of saturation. This behavior is similar to that of consolidated undrained cohesive soils subjected to triaxial compression (Bishop and Henkel, 1962). The Mohr diagram for the constant strain-rate tests on Sault Ste. Marie clay is shown in Figure 5-9, and indicates a cohesion value of 402 Psi and a zero friction angle, at a temperature of -12°C and a constant strain-rate of 3×10^{-3} in./in./min.

The stress-strain curves for constant axial strain-rate tests on sand-ice samples with a 64% sand volume concentration, at a temperature of -12°C, and constant confining pressures of 30 Psi, 60 Psi, and 90 Psi are shown in Figures 5-10a, 5-10b, and 5-10c. These figures also include the strain-time relation during the progress of each test.

The stress-strain curves for the sand-ice samples showed a peak value at a strain level of approximately 1.8%. The confining pressure showed a considerable effect on the value of the ultimate strength of the tested samples. The strength increased with higher value of confining pressure, showing an internal friction factor in strength. This is in agreement with the work by Goughnour (1967). A Mohr diagram for the constant axial strain-rate tests conducted on identical sand-ice samples, at a temperature of -12°C, is shown in Figure 5-11. Close linear agreement between the three plotted p ~ q values[1] indicates excellent duplication between samples. The diagram gives a cohesion value of 435 Psi, and angle of internal friction equal to 25°, for sand-ice samples at -12°C and a constant strain-rate of 3×10^{-3} in./in./min. Experimental data are given in the Appendix.

---

[1] $p = \frac{\sigma_1+\sigma_3}{2}$

$q = \frac{\sigma_1-\sigma_3}{2}$

Table 5-I. Differential Creep Test Results on Sault Ste. Marie Clay.

Axial Loading Psi	Confining Pressure σ_3, Psi	Major Princ. Stress σ_1,* Psi	Mean Stress σ_m, Psi	Stress Difference $D=\sigma_1-\sigma_3$, Psi	Creep Rate $\dot{\varepsilon}$, in./in./min.	
569	0	569	189.6	569	2.45×10^{-4}	
569	20	589	209.6	569	1.33×10^{-4}	Sample No.
569	40	609	229.6	569	9.45×10^{-5}	C-4
569	60	629	249.6	569	7.75×10^{-5}	γ_d=102.8 Pcf
569	80	649	269.6	569	6.48×10^{-5}	w=24.13%
569	100	669	289.6	569	5.33×10^{-5}	
677.95	0	677.95	225.98	677.95	2.01×10^{-4}	
677.95	30	707.95	255.98	677.95	1.26×10^{-4}	Sample No.
677.95	60	737.95	285.98	677.95	9.22×10^{-5}	C-1
677.95	90	767.95	315.98	677.95	6.58×10^{-5}	γ_d=102.2 Pcf
677.95	120	797.95	345.98	677.95	4.72×10^{-5}	w=24%
677.95	150	827.95	375.98	677.95	3.45×10^{-5}	
714.67	0	714.67	238.22	714.67	2.41×10^{-4}	
714.67	30	744.67	268.22	714.67	1.15×10^{-4}	Sample No.
714.67	60	774.67	298.22	714.67	8.29×10^{-5}	C-2
714.67	90	804.67	328.22	714.67	6.04×10^{-5}	γ_d=101.7 Pcf
714.67	120	834.67	358.22	714.67	4.59×10^{-5}	w=24.3%
714.67	150	864.67	388.22	714.67	3.25×10^{-5}	
782.25	0	782.25	260.75	782.25	3.15×10^{-4}	
782.25	30	812.25	290.75	782.25	1.14×10^{-4}	Sample No.
782.25	60	842.25	320.75	782.25	7.61×10^{-5}	C-3
782.25	90	872.25	350.75	782.25	5.31×10^{-5}	γ_d=102.9 Pcf
782.25	120	902.25	380.75	782.25	4.00×10^{-5}	w=24.33%
782.25	150	932.25	410.75	782.25	2.92×10^{-5}	

*In a triaxial type test σ_1 equal to the axial loading plus the confining pressure.

Table 5-II. Differential Creep Test Results on Sand-Ice Samples.

Axial Loading Psi	Confining Pressure σ_3, Psi	Major Princ. Stress σ_1,* Psi	Mean Stress σ_m, Psi	Stress Dif- $D=\sigma_1-\sigma_3$, Psi	Creep Rate $\dot{\varepsilon}$, in./in./min.	
660.62	0	660.62	220.20	660.62	1.38×10^{-4}	Sample No.
660.62	30	690.62	250.20	660.62	8.72×10^{-5}	S-1
660.62	60	720.62	280.20	660.62	6.18×10^{-5}	γ_d=107.5 Pcf
660.62	90	750.62	310.20	660.62	4.60×10^{-5}	w=19.42%
660.62	120	780.62	340.20	660.62	3.20×10^{-5}	Ice bulk density=
660.62	150	815.62	370.20	660.62	2.20×10^{-5}	0.915gm/cm^3
764.26	0	764.26	254.75	764.26	2.21×10^{-4}	Sample No.
764.26	30	794.26	284.75	764.26	1.38×10^{-4}	S-2
764.26	60	824.26	314.75	764.26	9.44×10^{-5}	γ_d=107.5 Pcf
764.26	90	854.26	344.75	764.26	7.26×10^{-5}	w=19.32%
764.26	120	884.26	374.75	764.26	4.77×10^{-5}	Ice bulk density=
764.26	150	914.26	404.75	764.26	3.44×10^{-5}	0.910gm/cm^3
815.93	0	815.93	271.97	815.93	2.38×10^{-4}	Sample No.
815.93	30	845.93	301.97	815.93	1.69×10^{-4}	S-3
815.93	60	875.93	331.97	815.93	1.15×10^{-4}	γ_d=107.5 Pcf
815.93	90	905.93	361.97	815.93	8.23×10^{-5}	w=19.26%
815.93	120	935.93	391.97	815.93	6.28×10^{-5}	Ice bulk density=
815.93	150	965.93	421.97	815.93	4.11×10^{-5}	0.907gm/cm^3
764.26	0	764.26	254.75	764.26	2.14×10^{-4}	Sample No.
764.26	30	794.26	284.75	764.26	1.45×10^{-4}	S-4
815.93	30	845.93	301.97	815.93	1.60×10^{-4}	γ_d=107.5 Pcf
815.93	60	875.93	331.97	815.93	1.08×10^{-4}	w=19.36%
						Ice bulk density=
						0.912gm/cm^3

*In a triaxial type test σ_1 equal to the axial loading plus the confining pressure.

Table 5-III. Stress, Temperature, and Creep Rate Test Results on Sand-Ice Samples.

Axial Loading Psi	Confining Pressure σ_3,Psi	Major Princ. Stress σ_1,Psi	Mean Stress σ_m,Psi	Stress Difference D,Psi	Creep Rate $\dot{\varepsilon}$, in./in./min. T=-10°C (1)	T=-12°C (2)	T=-14°C (3)	T=-18.1°C (4)
764.26	0	764.26	254.75	764.26	2.33×10^{-4}	2.21×10^{-4}	1.75×10^{-4}	1.25×10^{-4}
764.26	30	794.26	284.75	764.26	1.55×10^{-4}	1.38×10^{-4}	1.18×10^{-4}	8.65×10^{-5}
764.26	60	824.26	314.75	764.26	1.09×10^{-4}	9.44×10^{-5}	8.65×10^{-5}	6.31×10^{-5}
764.26	90	854.26	344.75	764.26	7.64×10^{-5}	7.26×10^{-5}	6.25×10^{-5}	4.30×10^{-5}
764.26	120	884.26	374.75	764.26	5.28×10^{-5}	4.77×10^{-5}	4.40×10^{-5}	3.09×10^{-5}
764.26	150	914.26	404.75	764.26	3.70×10^{-5}	3.44×10^{-5}	3.00×10^{-5}	2.20×10^{-5}

(1) Sample No. S-5, γ_d=107.5 Pcf, w=19.37%, and ice bulk density = 0.913 gm./cm^3.

(2) Sample No. S-2, γ_d=107.5 Pcf, w=19.32%, and ice bulk density = 0.910 gm./cm^3.

(3) Sample No. S-6, γ_d=107.5 Pcf, w=19.34%, and ice bulk density = 0.911 gm./cm^3.

(4) Sample No. S-7, γ_d=107.5 Pcf, w=19.40%, and ice bulk density = 0.914 gm./cm^3.

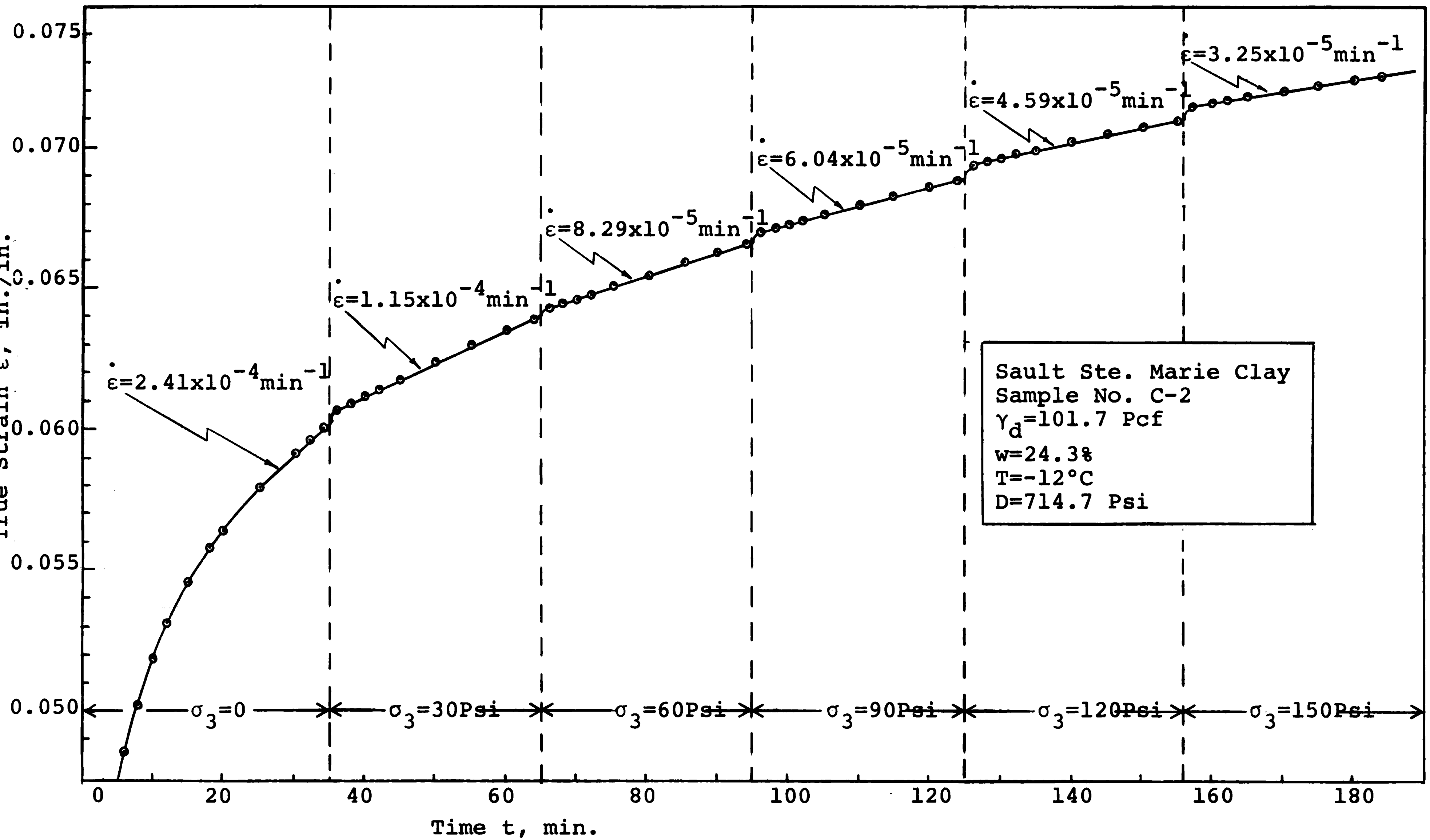

Figure 5-1A. Differential Creep Test on Sault Ste. Marie Clay, D Equal to 714.7 Psi.

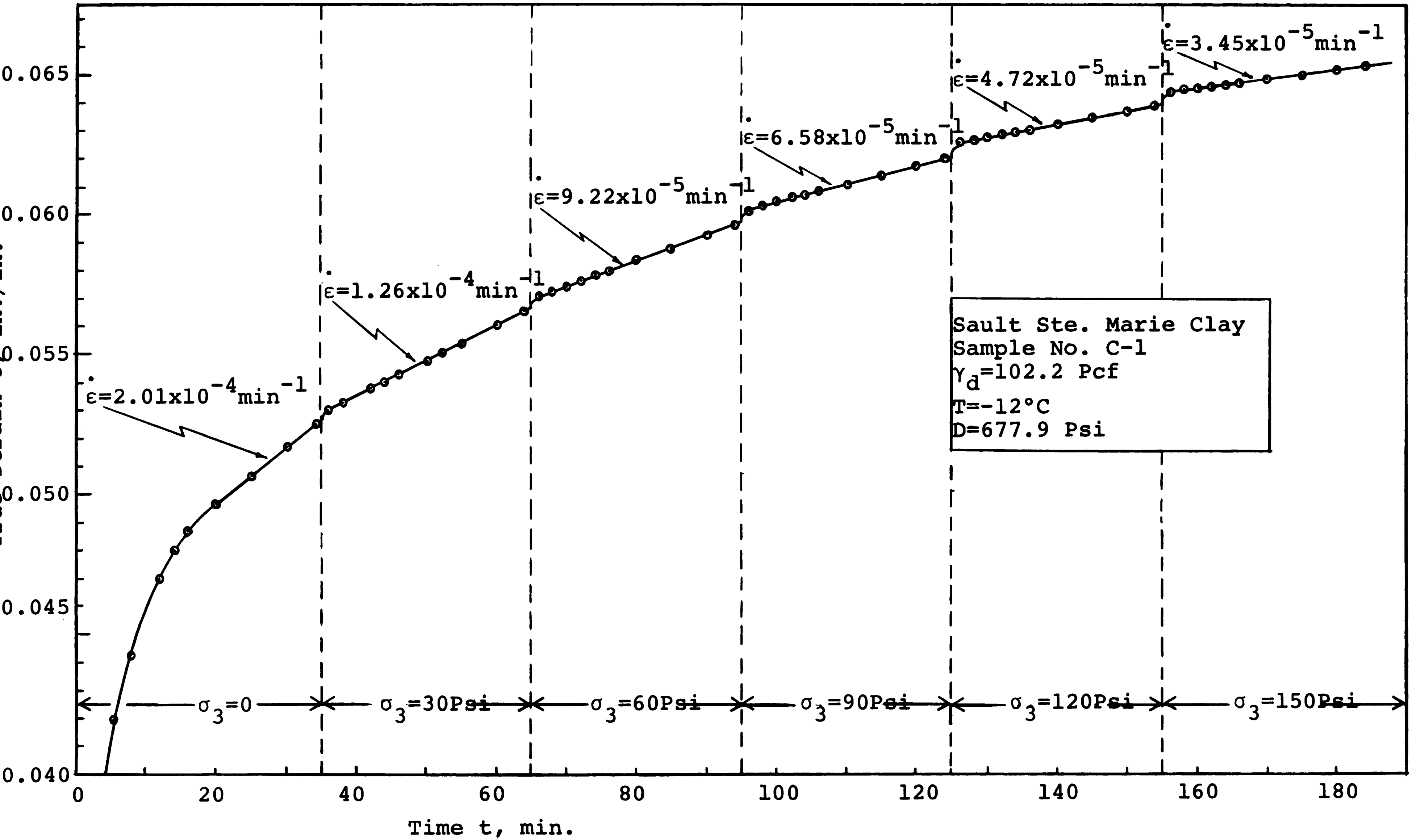

Figure 5-1B. Differential Creep Test on Sault Ste. Marie Clay, D Equal to 677.9 Psi.

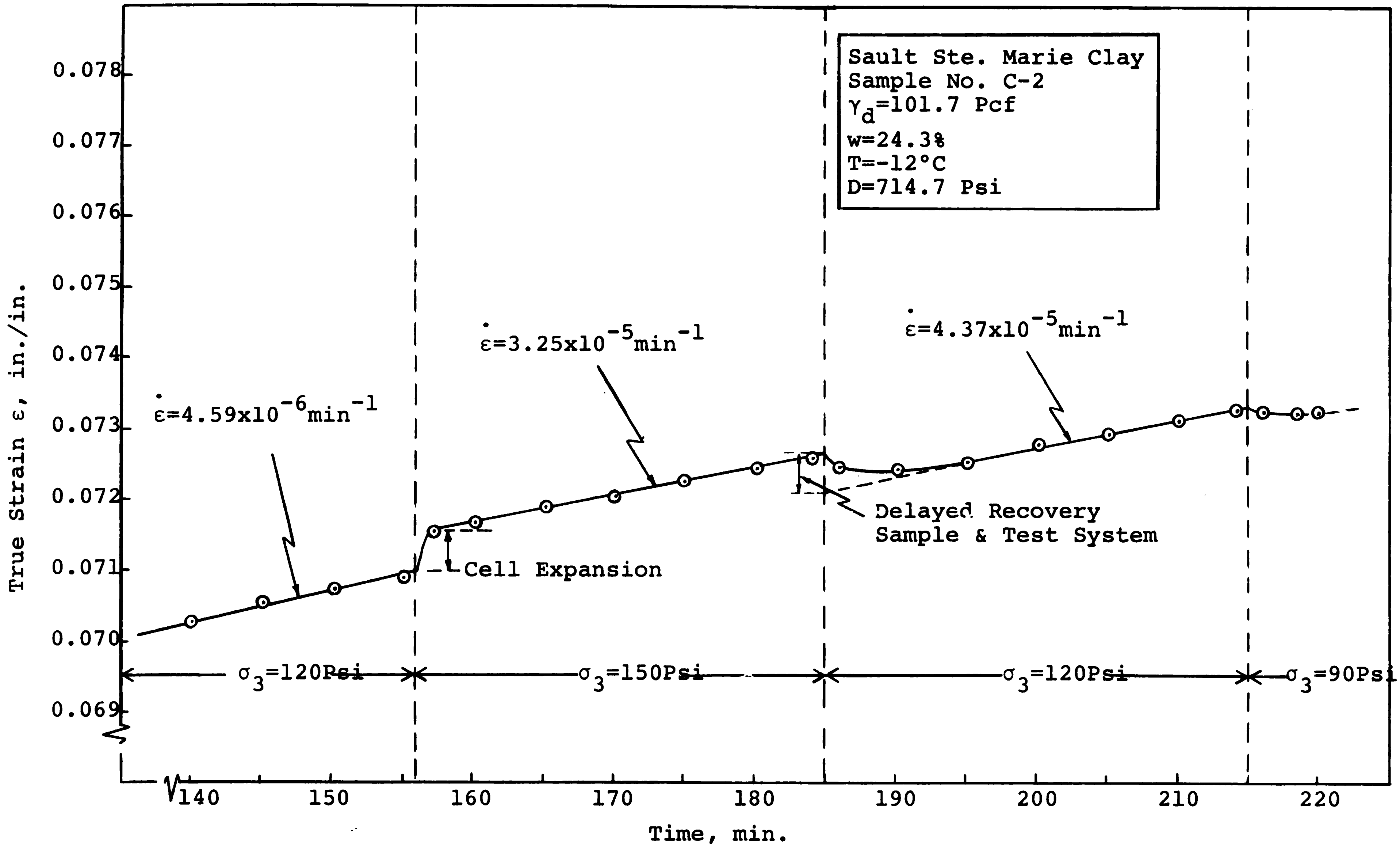

Figure 5-2. Strain ~ Time Relations During Increase and Decrease of Confining Pressure.

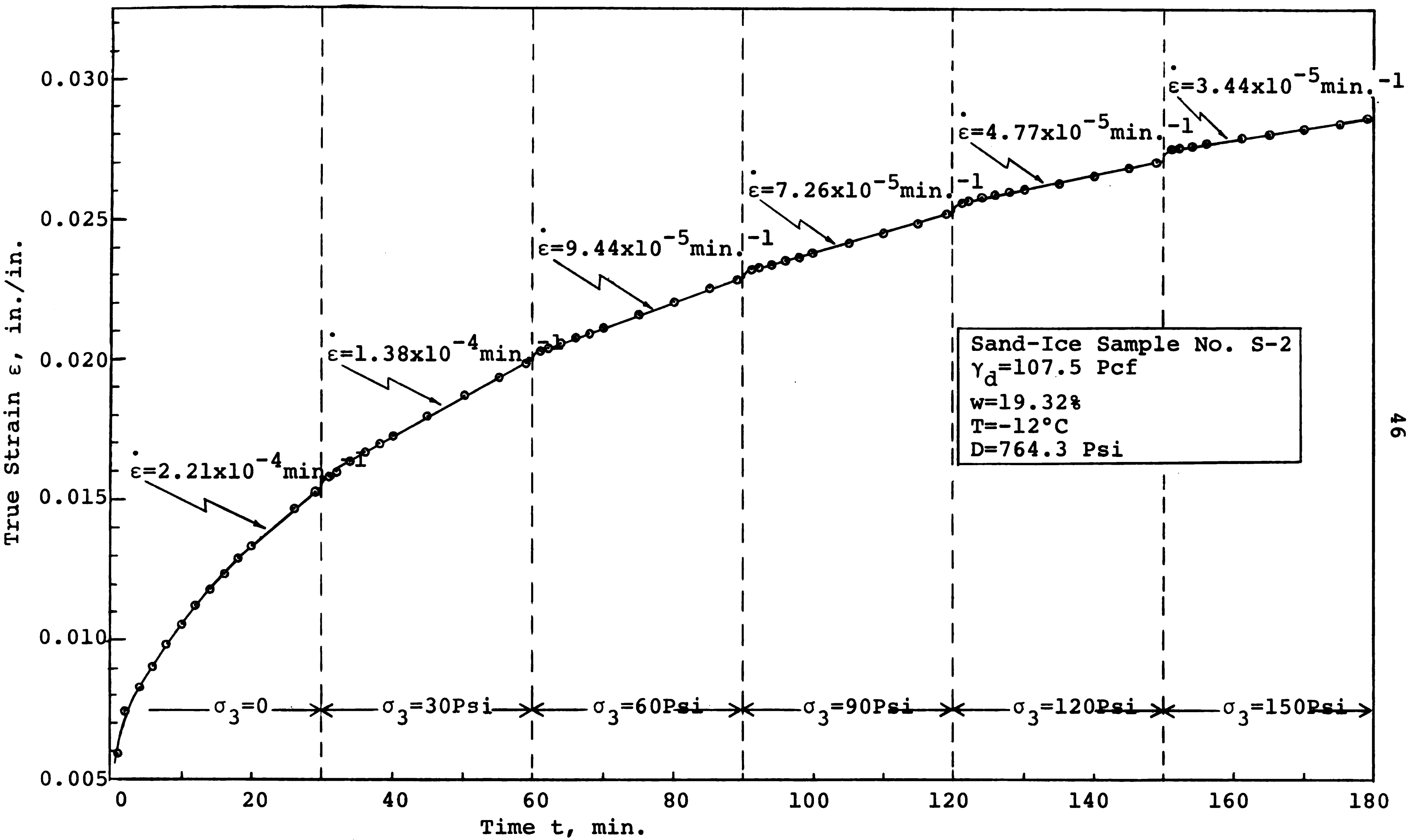

Figure 5-3A. Differential Creep Test on Sand-Ice Sample, D Equal to 764.3 Psi.

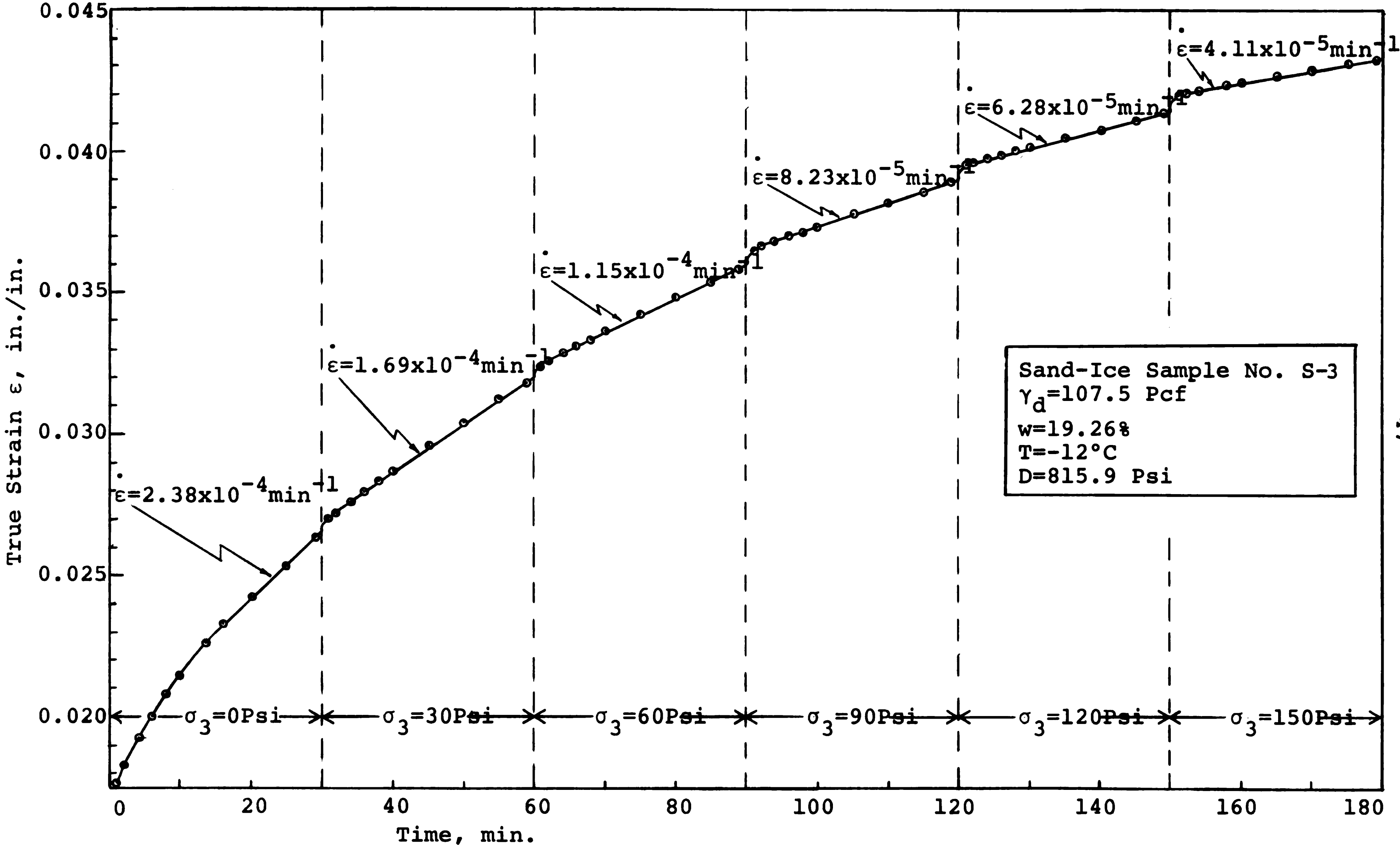

Figure 5-3B. Differential Creep Test on Sand-Ice Sample, D Equal to 815.9 Psi.

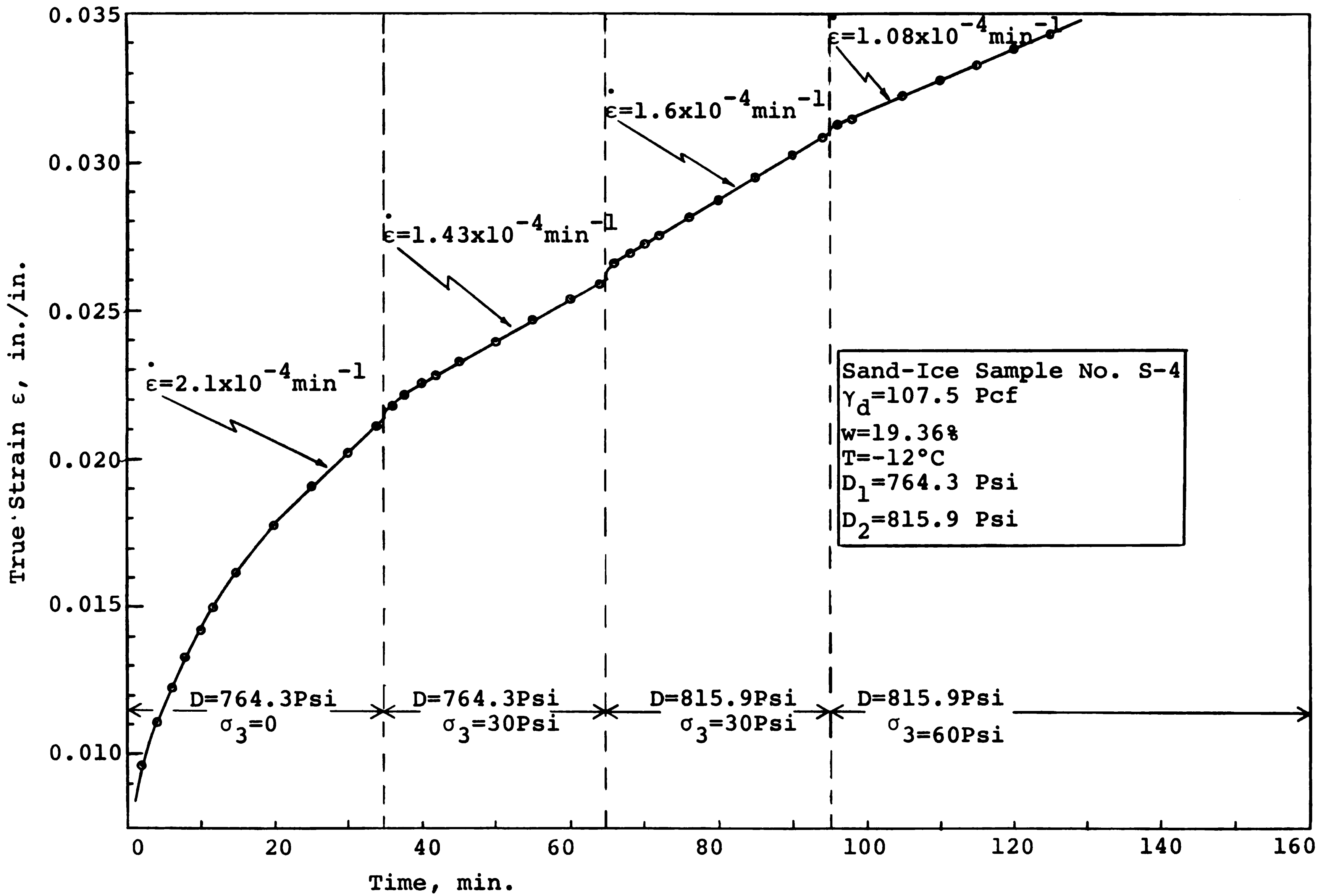

Figure 5-4. Differential Creep Test on Sand-Ice, D_1 Equal to 764.3 Psi and D_2 Equal to 815.9 Psi.

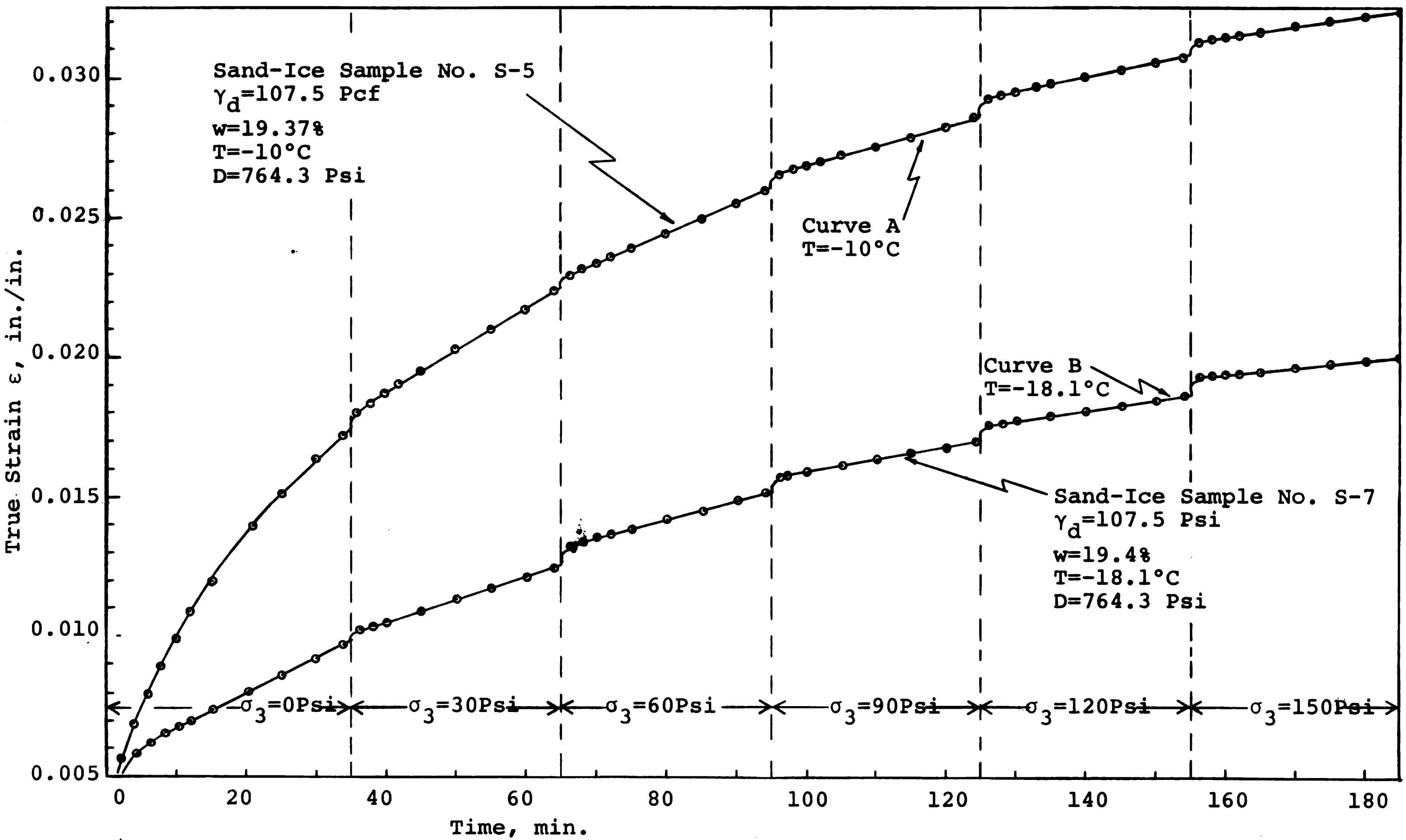

Figure 5-5. Differential Creep Test on Sand-Ice, (A) @ T=-10°C, (B) @ T=-18.1°C.

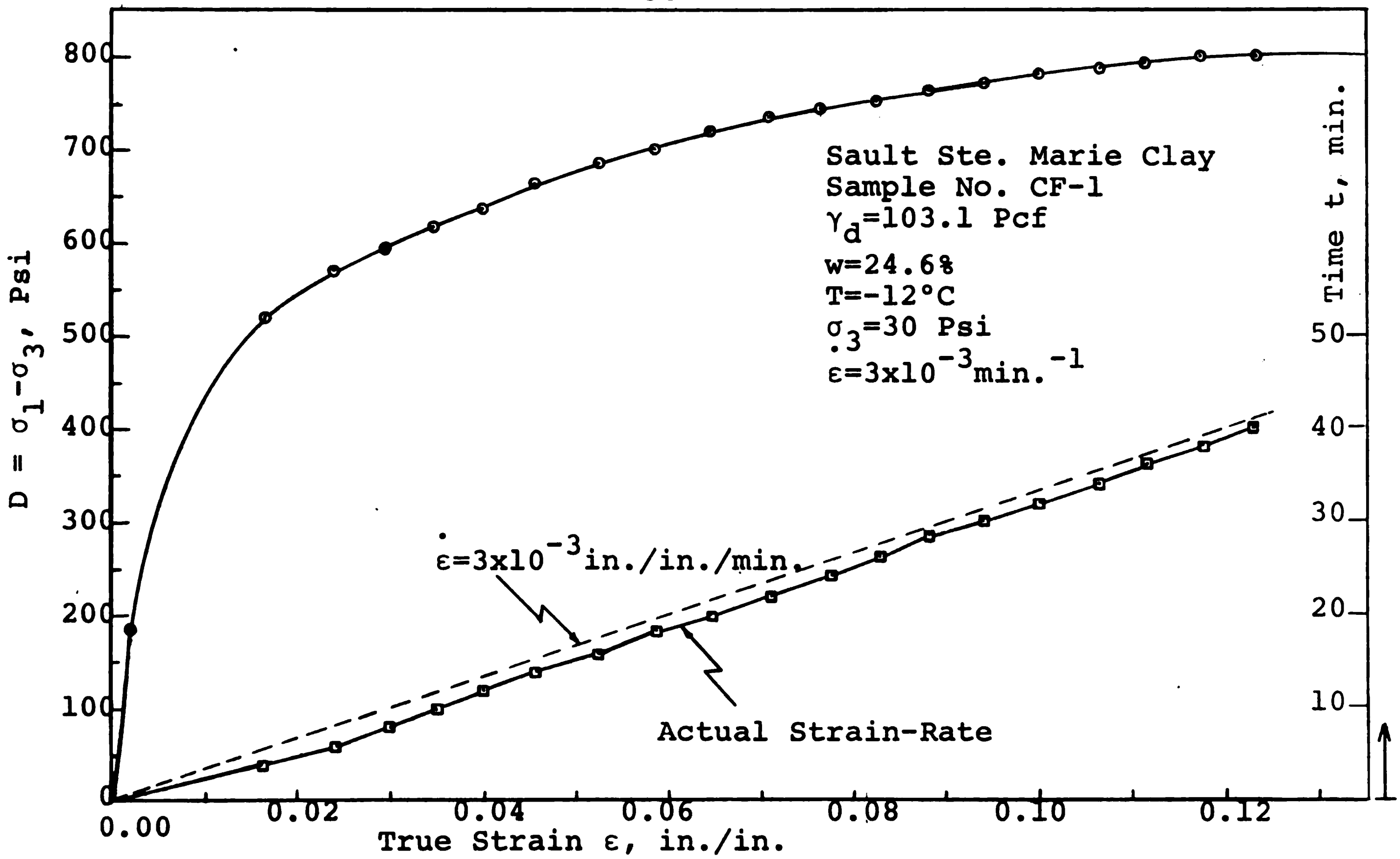

Figure 5-6. Stress ~ Strain and Strain ~ Time Curves for Sault Ste. Marie Clay, σ_3 Equal to 30 Psi.

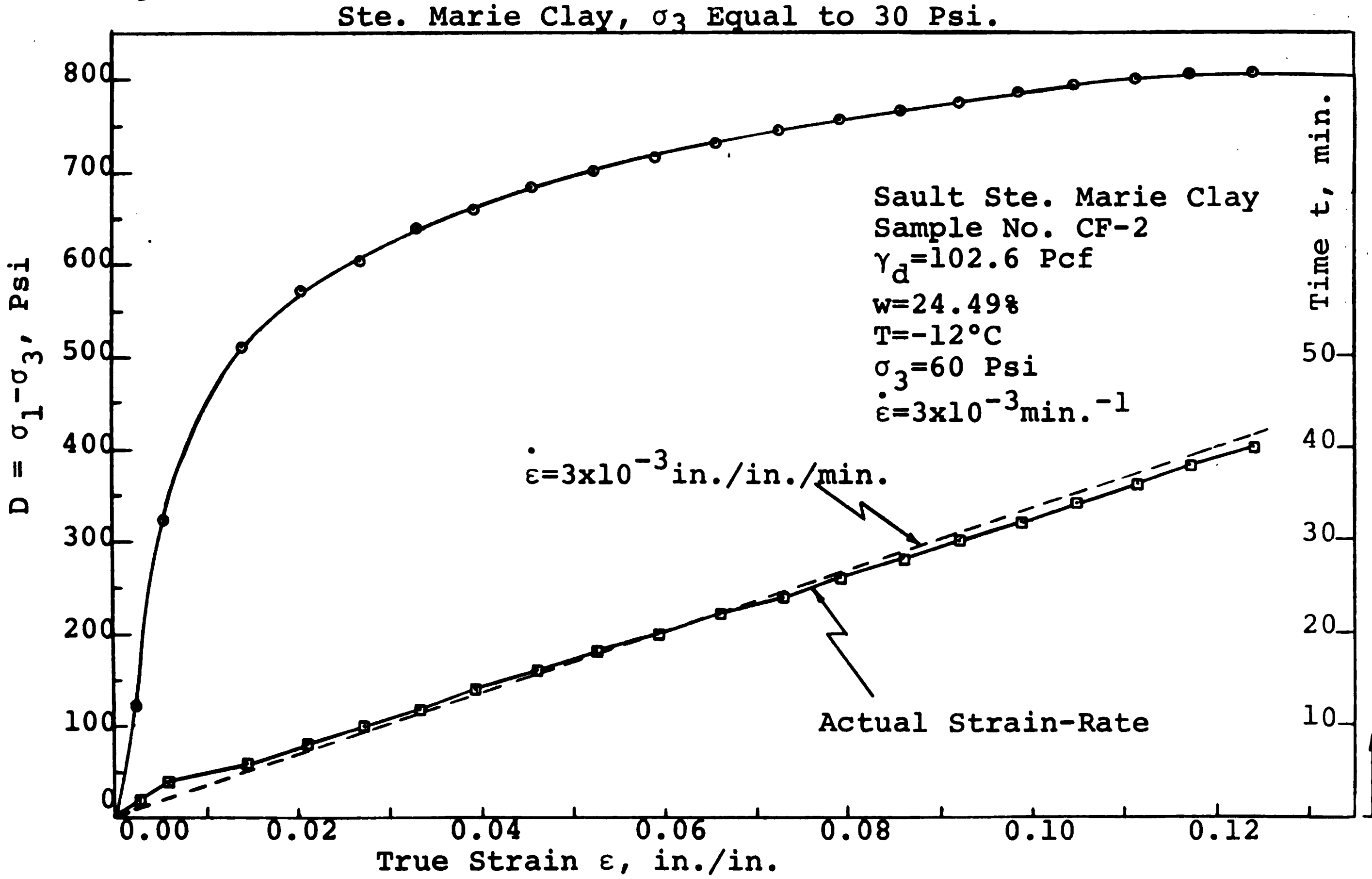

Figure 5-7. Stress ~ Strain and Strain ~ Time Curves for Sault Ste. Marie Clay, σ_3 Equal to 60 Psi.

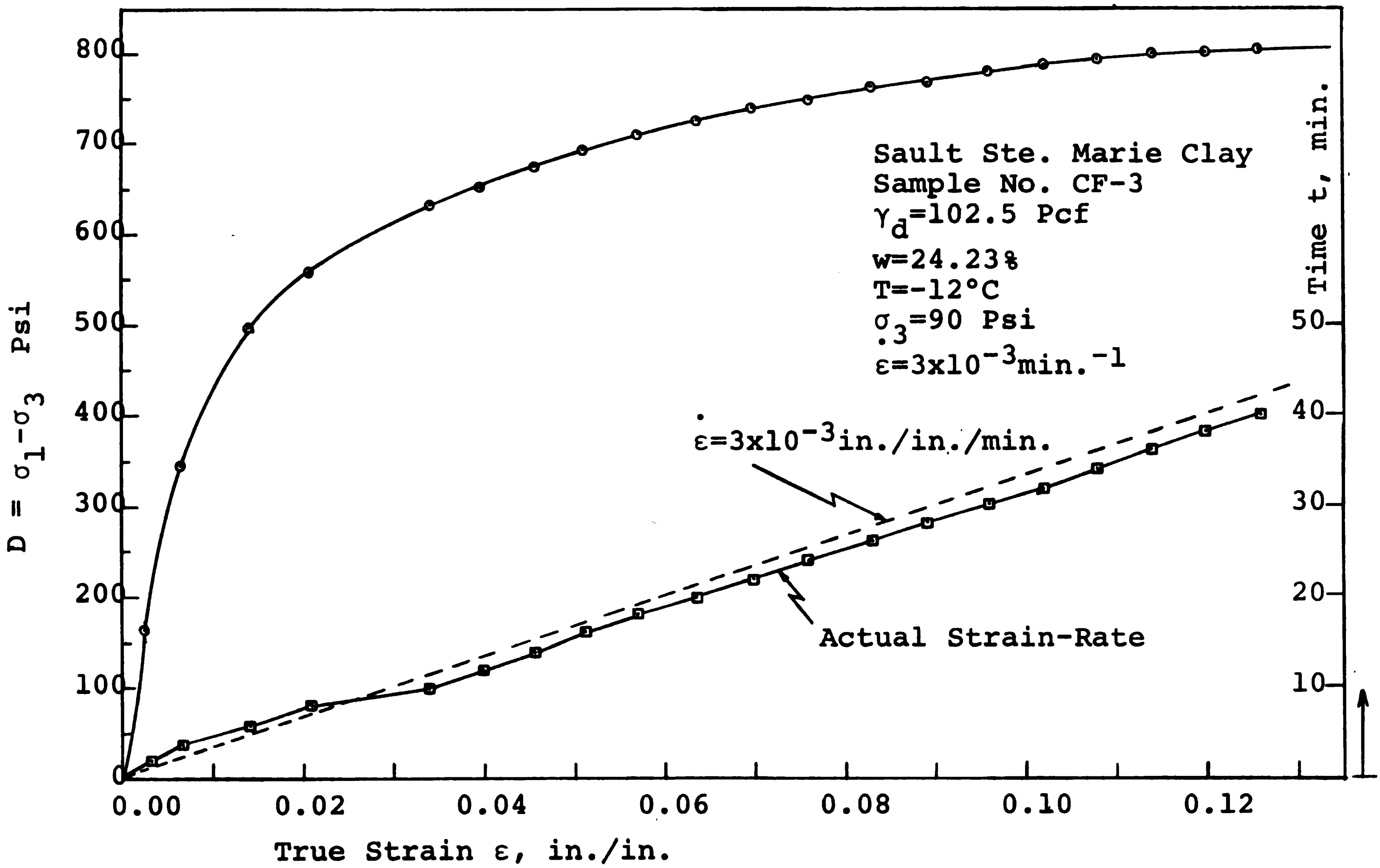

Figure 5-8. Stress ~ Strain and Strain ~ Time Curves For Sault Ste. Marie Clay, σ_3 Equal to 30 Psi.

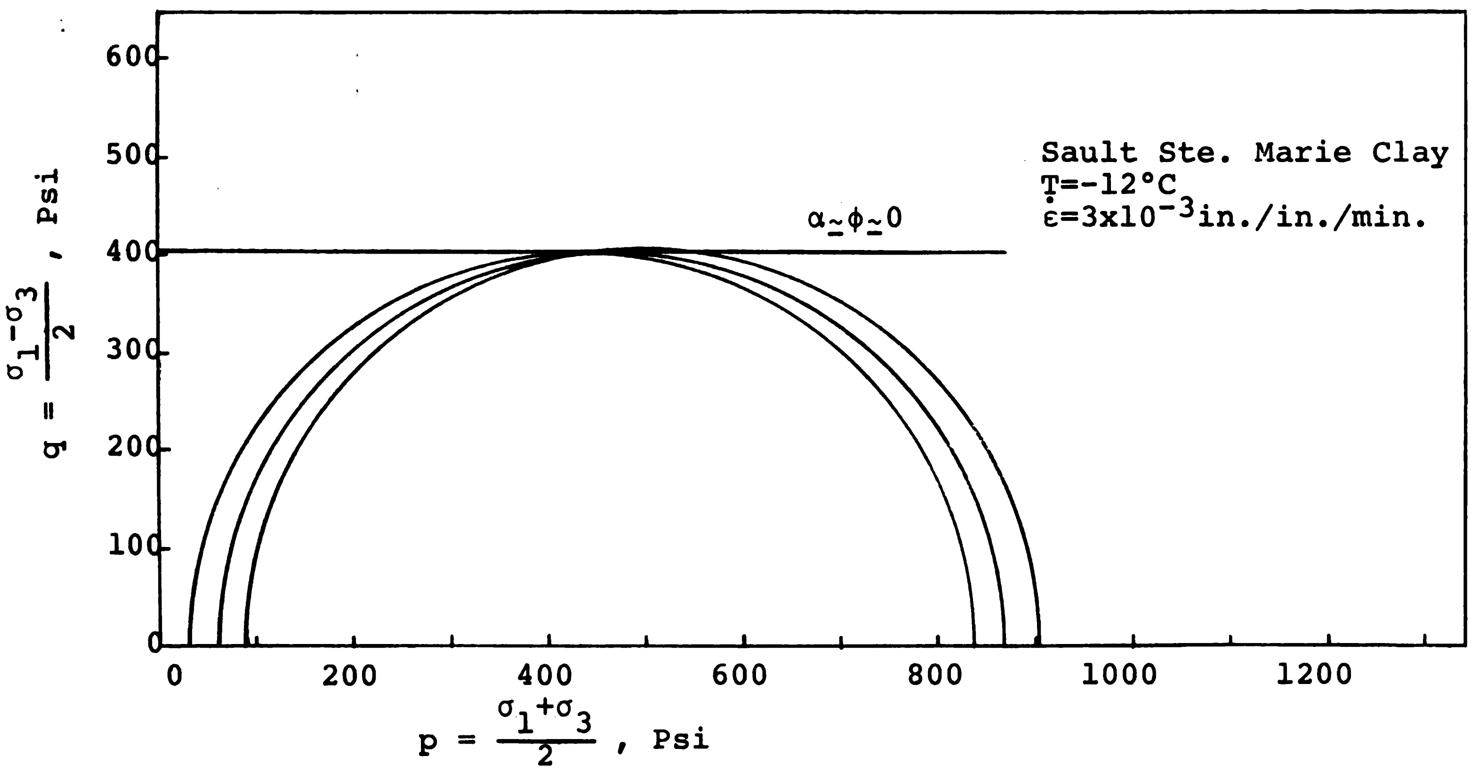

Figure 5-9. Mohr-Coulomb Plot and Modified Plot for Sault Ste. Marie Clay Samples.

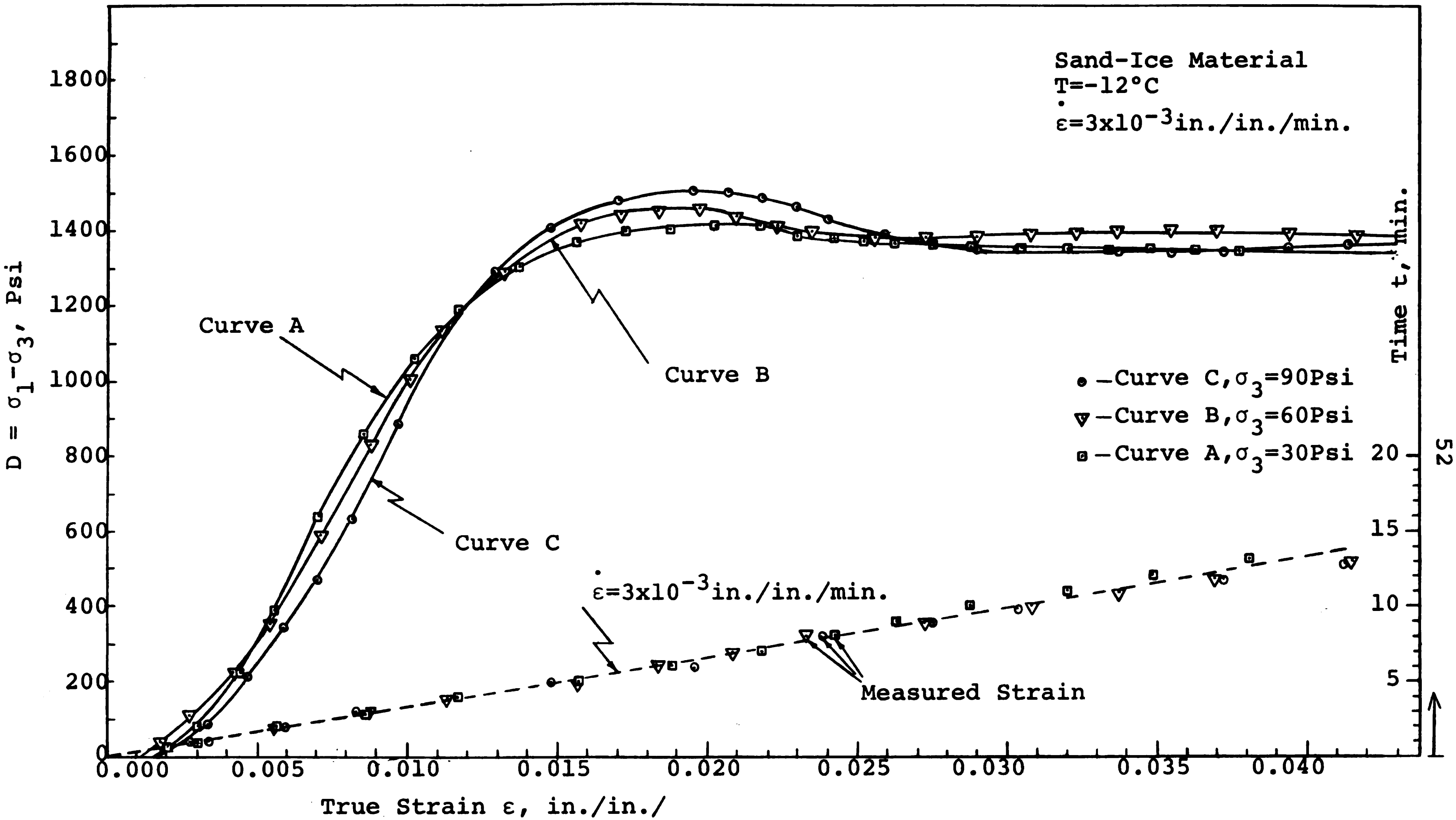

Figure 5-10. Stress ~ Strain Curves for Sand-Ice Samples, (A) σ_3 Equal to 30 Psi, (B) σ_3 Equal to 60 Psi, (C) σ_3 Equal to 90 Psi.

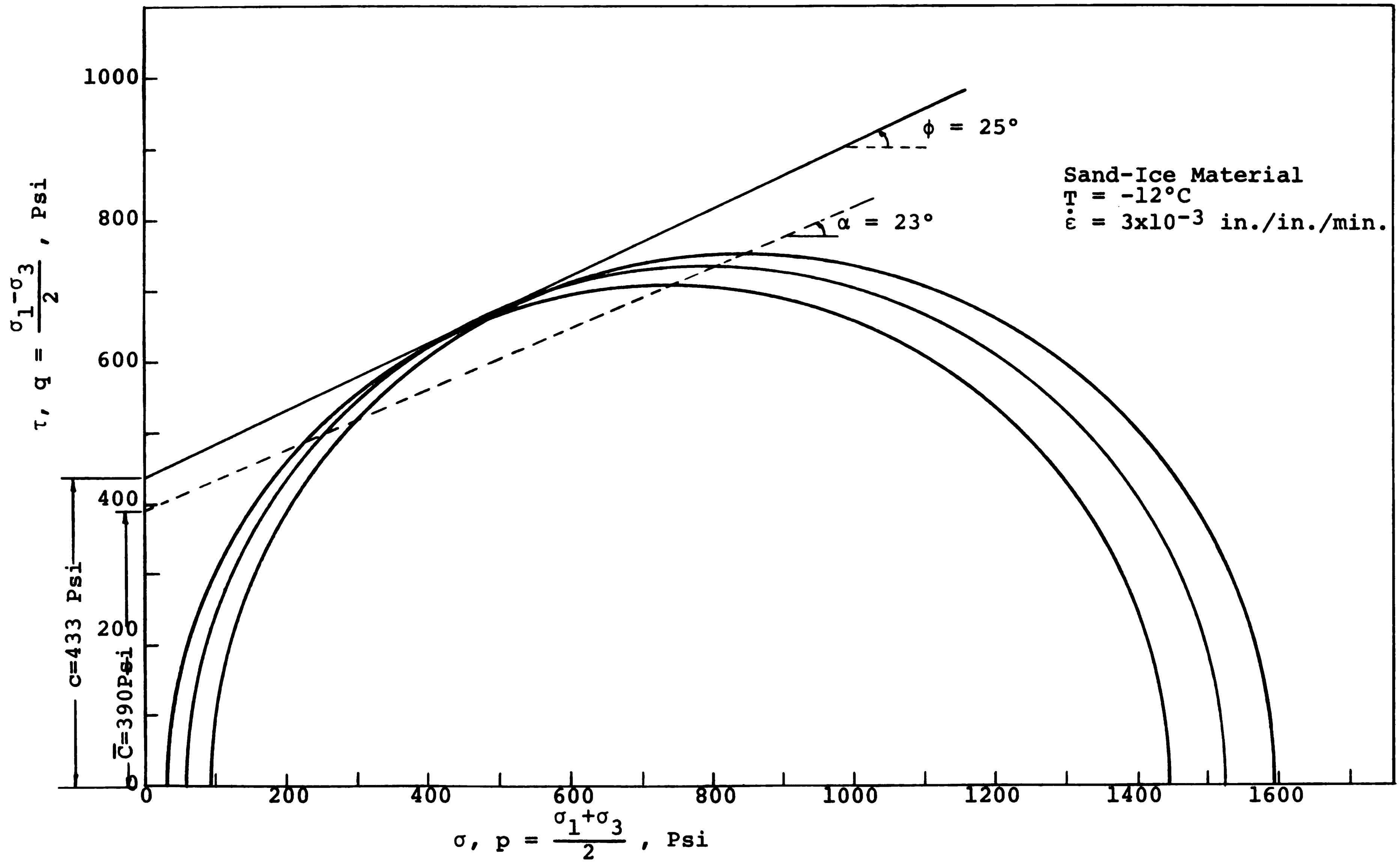

Figure 5-11. Mohr-Coulomb Plot and Modified Plot for Sand-Ice Samples.

CHAPTER VI

DISCUSSION AND PRESENTATION OF THEORY

The results of the differential creep tests conducted on frozen Sault Ste. Marie clay at a constant temperature of -12°C, summarized in Table 5-1, show a linear relationship between the logarithm of the steady state creep rate $\dot{\varepsilon}$ and a stress term Σ. The stress term $\Sigma = D - \sigma_m$ is a function of both the deviatoric component and the hydrostatic component of stress, where D is the stress difference,[1] and σ_m is the hydrostatic or the mean normal stress.[2] This linear relation between log $\dot{\varepsilon}$ and Σ is shown in Figure 6-1 as a family of linear curves. Each corresponds to a different constant value of stress difference D. The equation representing this linear relation may be expressed in the following form:[3]

---

[1] $D = \sigma_1 - \sigma_3$

$= 3/2\ (\sigma_1 - \sigma_m)$, since $\sigma_2 = \sigma_3$ in the triaxial test apparatus.

[2] $\sigma_m = 1/3\ (\sigma_1 + \sigma_2 + \sigma_3)$

$= 1/3\ (\sigma_1 + 2\sigma_3)$.

[3] log: designates the common logarithm for which the base is 10. ℓn: designates the natural logarithm for which the base is e = 2.71828.

$$\log \dot{\varepsilon} = (m \log e)\ \Sigma + \log b$$

which implies that the creep rate $\dot{\varepsilon}$ is an exponential function of the stress term Σ, at constant temperature, and which can be put in the following form:

$$\dot{\varepsilon} = b \exp (m\ \Sigma) \qquad @\ T = \text{const.} \qquad (6\text{-}1)$$

where m is the absolute value of slope of the straight line on the log-creep rate verses Σ plot, and b is the projected value of creep rate at zero Σ on the same plot. b has no physical meaning. The value of m was determined graphically from Figure 6-1 for frozen Sault Ste. Marie clay at a constant temperature of -12°C. A nearly linear relationship is found between log b and the stress difference D for the differential creep tests on the Sault Ste. Marie clay, which implies that the b value approximates an exponential function of the stress difference D for differential creep tests on frozen clay. This relation is shown in Figure 6-3, and could be presented in the following form:

$$b = C \exp (n\ D) \qquad @\ T = \text{const.} \qquad (6\text{-}2)$$

The parameters C and n are constants at a constant test temperature and could be evaluated graphically from Figure 6-3. By substituting the exponential function b (equation 6-2) for the b value in equation 6-1 we obtain

$$\dot{\varepsilon} = C \cdot \exp\ (n\ D) \cdot \exp\ (m\ \Sigma) \qquad @\ T = \text{const.} \qquad (6\text{-}1a)$$

since $\Sigma = D - \sigma_m$, if we let $N = n + m$, then:

$$\dot{\varepsilon} = C \cdot \exp\ (N\ D) \cdot \exp\ (-m\ \sigma_m) \qquad @\ T = \text{const.} \qquad (6\text{-}3)$$

For frozen Sault Ste. Marie clay at a temperature of -12°C, equation 6-3 becomes:

$$\dot{\varepsilon} = (2.77 \times 10^{-4}) \cdot e^{(0.00268)D} \cdot e^{-(0.01049)}\ {}_{m}$$

$$@\ T = -12°C \qquad (6\text{-}4)$$

$\dot{\varepsilon}$ is measured in inch/inch/minute, D and σ_m in Psi. Knowing the stress conditions and the parameters C, N, and m for a frozen clay, we can use equation (6-3) to estimate the steady state creep rate for that clay at a constant temperature, as long as the applied stresses are within the range which exhibits a linear relation between log $\dot{\varepsilon}$ and Σ. Equation (6-3) indicates that the creep rate of frozen clay, at a constant temperature and the stress-history used, increases exponentially with the increase in stress difference D, and decreases exponentially with the increase in mean stress σ_m.

The results of the differential creep tests conducted on sand-ice samples, at a constant temperature of -12°C, showed the existence of a linear relationship between the logarithm of the steady state creep rate and the stress term Σ, which indicates a similar behavior to that of the creep of frozen clays. This linear relation between log $\dot{\varepsilon}$ and Σ is shown in Figure 6-2 as a family of curves, each corresponding to a different value of stress difference D. Figure 6-2 indicates that the creep rate of sand-ice samples, at a constant temperature, is an exponential function of the stress term Σ, and could be described by a mathematical expression similar to the one used to describe the creep behavior of frozen clay in equation (6-1), except that the b and m parameters assume different values. m can be evaluated from Figure 6-2. Then, for a sand-ice material of 64% sand by volume concentration, at a constant temperature of -12°C, equation (6-1) becomes:

$$\dot{\varepsilon} = b_1 \; e^{(0.01206)\Sigma} \qquad @ \; -12°C \qquad (6\text{-}5)$$

The log b_1 verses D plot, shown in Figure 6-4, exhibited a nearly linear relation, indicating that b_1 is an exponential function of D at a constant temperature, and could be represented in a form similar to equation 6-2. For a sand-ice material at -12°C , the linear relation in Figure 6-4 between log b_1 and D can be expressed as:

$$b_1 = (9.103 \times 10^{-6}) \; e^{-(0.0398)D} \qquad @ \; T = -12°C \qquad (6\text{-}6)$$

By substituting equation (6-6) for b_1 in equation 6-5 we get:

$$\dot{\varepsilon} = (9.103\text{x}10^{-6}) \cdot e^{-(0.00398)D} \cdot e^{(0.01206)\Sigma}$$

$$@ \; T = -12°C \qquad (6\text{-}7)$$

since $\Sigma = D - \sigma_m$, then:

$$\dot{\varepsilon} = (9.103 \times 10^{-6}) \cdot e^{(0.00808)D} \cdot e^{-(0.01206)\sigma_m}$$

$$@ \; T = -12°C \qquad (6\text{-}7a)$$

The form of equation (6-7a) is the same as that of equation (6-3). It describes the steady state deformation of a 64% volume concentration sand-ice material at a constant temperature of -12°C, and for the stress-history imposed on the test samples.

Equation (6-3) describes the steady state deformation at a constant test temperature for both a frozen clay system and a frozen saturated sand system. At a temperature of -12°C, the graphical solution of equation (6-3) is shown in Figure 6-1 for a frozen Sault Ste. Marie clay, and in Figure 6-2 for a frozen saturated sand. It is obvious from Figure 6-1 and 6-2 that the slope of the relationship, in each case, is essentially independent of the creep stress, implying that the parameter m is a constant, and therefore is a property of the material. An increase in stress serves only to shift the line vertically upwards. Figure 6-5 shows a semilog plot of the $\dot{\varepsilon} \sim \Sigma$ curve for two differential creep tests, the first on a frozen saturated sand sample, and the second on a frozen

Sault Ste. Marie clay. Both tests were conducted at the same test temperature of -12°C, and under relatively close values of stress difference D of 660.6 Psi and 677.9 Psi respectively. The curve for the frozen sand exhibits a higher value of slope (m = 0.01206) than that of the frozen clay (m = 0.01049). This is explained by the theory of the equilibrium state between water and ice in frozen soils (Tsytovich, 1960), since frozen clays generally contain a considerably larger amount of unfrozen water in comparison to sands, thus exhibiting less resistance to external loading.

Differential creep test No. S-4 was conducted on a sand-ice sample at -12°C, in which the deviatoric stress was increased by increasing the axial loading during the test. The measured steady state creep rates corresponding to the various loading conditions are compared with the predicted creep rates by equation 6-3, for the same loading conditions, in Figure 6-6. It is evident from Figure 6-6 that there is an agreement, to a considerable degree, between the predicted creep rates by equation 6-3 and the measured creep rates for a test in which the deviatoric stress is changed during the test.

The fundamental assumptions of the usual theory of elastoplastic deformation in isotropic hardening metals (Hill, 1950) imply that the change of body shape is caused only by deviatoric stresses and does not depend on the average normal stress (hydrostatic pressure σ_m), and the change in volume is caused only by hydrostatic pressure and does not depend on the deviatoric stresses. In this theory based on the Mises yield condition, during a proportional straining (one in which the plastic strain components maintain their ratios), the relationship between the equivalent stress $\bar{\sigma}$ (4) and the equivalent strain $\bar{\varepsilon}$ (5) does not depend on the state of stress of the body, i.e., the $\bar{\sigma}$ - $\bar{\varepsilon}$ diagram is invariant to this state. However, the indicated principle holds true only for bodies similarly resisting extension and compression, which frozen soils do not. It has been established (Vialov, 1965d) that, for soils, the relation between $\bar{\sigma}$ and $\bar{\varepsilon}$ at different values of mean stress σ_m is represented by a family of curves, each of which corresponds to its own value of σ_m. Thus, for frozen soils, just as for other bodies differently resisting extension and compression, equivalent strain will depend not only on $\bar{\sigma}$ but also on mean stress σ_m. In creep problems the time t becomes another factor. Existing creep theories do not take the influence of mean stress σ_m into consideration. The results of tests conducted in

---

(4) $\bar{\sigma} = \sqrt{3J_2'}$, J_2' is the second invariant of deviatoric stress, $J_2' = \frac{1}{6}\left[(\sigma_1-\sigma_2)^2 + (\sigma_2-\sigma_3)^2 + (\sigma_3-\sigma_1)^2\right]$

(5) $\bar{\varepsilon} = \left\{\frac{2}{3}\left[(\varepsilon_1-\varepsilon_2)^2 + (\varepsilon_2-\varepsilon_3)^2 + (\varepsilon_3-\varepsilon_1)^2\right]\right\}^{1/2}$

this study indicate that the mean stress does affect the creep rate of frozen soils. Thus any deformation equation should be a function of σ_m:

$$f\ (\bar{\sigma},\ \sigma_m,\ \dot{\varepsilon}) = 0$$

for a triaxial type test is:

$$\bar{\sigma} = \sigma_1 - \sigma_3 = D$$

and equation (6-3) would suggest a deformation criterion of the following form, at a constant temperature:

$$f\ (\dot{\varepsilon}) = f_1(\bar{\sigma}) - f_2(\sigma_m) \qquad @\ T + \text{const.} \qquad (6\text{-}8)$$

Temperature is one of the most important factors influencing the deformation of frozen soils. If we consider the results of the differential creep tests on sand-ice samples under a constant deviatoric stress and at different test temperatures, as shown in Figure 6-7, it is apparent that a linear relation exists between the logarithm of the creep rate and the stress term Σ. The slope of this linear relation is equal to that of equation (6-5), which describes the creep deformation of the same material at a constant temperature and different values of deviatoric stress. This relation between log $\dot{\varepsilon}$ and Σ can be expressed as:

$$\dot{\varepsilon} = b_2 \exp\ (m\ \Sigma) \qquad @\ D = \text{const.} \qquad (6\text{-}9)$$

m is equal to (0.01206) for a creep test on sand-ice sample under a constant stress difference D = 764.3 Psi. The slopes of equation (6-5) and (6-9) in a semilog plot are equal (m = 0.01206). This indicates that the parameter m is neither a function of the stress difference D nor of the test temperature. The plot of log b_2 verses the reciprocal of test temperature T, measured in absolute units and shown in Figure 6-8, indicates the existence of a nearly linear relationship between log b_2 and $\frac{1}{T}$. This relation could be described by the following function:

$$b_2 = C' \cdot \exp\left(-\ell \cdot \frac{1}{T}\right) \qquad @\ D = \text{const.} \qquad (6\text{-}10)$$

where ℓ is the slope of the linear relation between log b_2 and $\frac{1}{T}$, which can be evaluated graphically. From Figure 6-8, ℓ = 4273.75 for creep tests conducted on sand-ice samples under a constant stress difference D = 764.3 Psi. Substituting equation (6-10) for b_2 in equation 6-9, we get:

$$\dot{\varepsilon} = C' \cdot \exp\left(-\ell\ \frac{1}{T}\right) \cdot \exp\left(m\ \Sigma\right) \quad @\ D = \text{const.} \ (6\text{-}11)$$

For creep tests on sand-ice samples under a constant stress difference D = 764.3 Psi, C', m, and ℓ can be evaluated graphically from Figures 6-7 and 6-8. Thus equation (6-11) becomes:

$$\dot{\varepsilon} = (5.623) \cdot e^{(-4273.75/T)} \cdot e^{(0.01206\Sigma)}$$

$$@\ D = 764.3 \text{ Psi} \qquad (6\text{-}11a)$$

Equation (6-11a) can be used to estimate the creep rate of sand-ice system under a constant stress difference D = 764.26 Psi, and it implies that, at a constant D, the creep rate is an exponential function of the reciprocal of test temperature. This confirms previous work that the creep phenomenon of frozen soil is a thermally activated process (Andersland and Akili, 1967). The most significant factor determining the strength properties of a frozen soil is the value of its temperature below freezing. The physical reasons for the increase of strength of a frozen soils with the decrease of its tempeature are: the freezing of new portions of water in the voids, and the change in quality of ice properties as a result of a decrease of mobility of hydrogen atoms in the crystalline lattice of ice.

Equation (6-1a) or (6-3) describes the creep rate at a constant temperature $T = T_1$, while Equation (6-11) describes the creep rate at a constant stress difference $D = D_1$. To combine the effect of both stress difference and test temperature, and considering equations (6-1a) and (6-11), we may suggest an equation in the following form:

$$\dot{\varepsilon} = A \cdot \exp\ (n\ D) \cdot \exp\ (-\ell \cdot \frac{1}{T}) \cdot \exp\ (m\ \Sigma) \qquad (6\text{-}12)$$

For equation (6-12) to combine the effect of both stress difference and test temperature, it has to confirm with equations6-1a at $T = T_1$, and with equation (6-11) at $D = D_1$:

At $T = T_1$, equation (6-12) becomes:

$$\dot{\varepsilon} = A\, e^{nD} \cdot e^{-\ell/T_1} \cdot e^{m\Sigma} \qquad @\ T = T_1$$

while equation (6-1a) is:

$$\dot{\varepsilon} = C \cdot e^{nD} \cdot e^{m\Sigma} \qquad @\ T = T_1$$

$$\therefore\ A = C \cdot e^{\ell/T_1}$$

For a sand-ice sample at a temperature of -12°C ($\frac{1}{T}$ = 0.00383): C = (9.103×10^{-6}), and ℓ = 4273.75.

$$A = 2.06715$$

At $D = D_1$, equation (6-12) becomes:

$$\dot{\varepsilon} = A\, e^{nD_1}\ e^{-\ell/T}\ e^{m\Sigma}$$

while equation (6-11) is:

$$\dot{\varepsilon} = \overline{C}\, e^{-\ell/T} \cdot e^{m\Sigma}$$

$$\therefore\ A = \overline{C}\, e^{-nD_1}$$

For sand-ice material at D_1 = 764.3 Psi: $\overline{C}$ = 5.623, and n = 0.00398.

$$\therefore\ A = 2.07084$$

The values of A determined in both conditions, at $T = T_1$ and $D = D_1$ for sand-ice material, appear to be approximately equal. Thus, considering possible experimental errors, A can be assumed constant for this range of creep stresses and temperatures, and is therefore a property of the material. However, A in general should be considered as a function of stress, temperature, and structure of the material. Since $\Sigma = D - \sigma_m$ and if we let $N = n + m$, equation (6-12) becomes

$$\dot{\varepsilon} = A \cdot \exp(ND) \cdot \exp(-\ell/T) \cdot \exp(-m\sigma_m) \qquad (6\text{-}13)$$

For frozen saturated sand with a 64% volume concentration of sand, equation (6-13) becomes:

$$\dot{\varepsilon} = (2.07) \cdot e^{0.00808D} \cdot e^{(-4273.75/T)} \cdot e^{-(0.01206)\sigma_m}$$

The large body of experimental data indicates that the creep rate, for materials in general, is given by the equation (Conrad, 1961):

$$\dot{\varepsilon} = \sum_i A_i\ (\sigma,T,S)\ e^{-\Delta H_i(\sigma,T,S)/RT} \qquad (6\text{-}14)$$

where A_i is the frequency factor and ΔH_i is the activation energy of one of a number of deformation mechanisms. A_i and ΔH_i may depend on the stress σ, temperature T, and structure S. Equation (6-13) describing the creep deformation of frozen soil is in agreement with the general deformation equation 6-14.

Since frozen soils possess clearly defined rheological properties, their strength is time dependent. In the steady state region of the creep curves, the deformation increases at a constant rate, and eventually reaches the tertiary creep (failure). Considering the creep tests carried out, at a constant temperature, on frozen clay and frozen saturated sand, which are shown in Figures 6-1 and 6-2, for a specific creep rate we note that there are several Σ values, each corresponding to a different creep test. Since the stress difference D for each test is known, we can determine the values of major and minor principal stresses σ_1 and σ_3, for each test, that correspond to a specific creep rate. Then, using these stress values a sketch can be prepared showing the modified Mohr plot (Lambe, 1967) which corresponds to a specific creep rate. This modified plot is shown in Figure 6-9 for frozen Sault Ste. Marie clay at -12°C, and in Figure 6-10 for a frozen saturated sand, at the same temperature. In Figure 6-9 and 6-10, the portion of the plot which corresponds to low stresses is neglected, since at that stress level, a steady state deformation region does not exist (damped creep). The strength of frozen soils is generally represented by a cohesion term and a friction term, and can be represented by two parameters, the equivalent cohesion C and the equivalent friction angle ϕ. Figure 6-9 indicates that the equivalent friction angle ϕ appears to remain constant with change in creep rate, at constant temperature, while the equivalent cohesion C decreases with a slower creep rate, implying the dependence of C on time. Cohesion of course depends on temperature too. The variation in the strength of frozen clay soil is influenced primarily by the rheological properties of ice and unfrozen water.

In Figure 6-10 the modified plot of a sand-ice material at -12°C, represents more clearly defined envelopes corresponding to different creep rates. The equivalent angle of friction ϕ appears to be constant, but the equivalent cohesion C decreased with a lower creep rate. The equivalent angle of friction ϕ for sand-ice system at these low creep rates was approximately 10 degrees higher than the friction angle of the same material at a relatively fast constant strain-rate tests shown in Figure 5-11, while the cohesion is considerably less. This implies that the equivalent angle of friction ϕ could be considered independent of time and temperature, therefore it is a property of the material. Since sands in unfrozen state do not exhibit any cohesion, the cohesion term exhibited in the frozen state is primarily due to the ice content, thus the cohesion in frozen saturated sand is controlled by the properties of ice. For simplification, we could consider the strength of frozen soil as:

$$\tau = C\ (T,L) + P \tan \phi$$

in which C is a function of time and temperature, and ϕ is a function of soil type.

The constant axial strain-rate tests indicate that at a relatively fast strain-rate (3×10^{-3} min^{-1}), frozen soils exhibit a much higher strength than at a slow strain-rate, therefore confirming previous works. No attempt was made to conduct compression tests at another fast strain-rate, since it is generally accepted that the ultimate strength of a frozen soil increases with increase in strain-rate (Goughnour, 1967). The constant axial strain-rate tests were conducted on both frozen Sault Ste. Marie clay and frozen saturated sand to determine the ultimate strength of these materials, which have been used in this study, at a fast strain rate, and to determine the effect of confining pressure on the ultimate strength of the frozen soil, in an effort to determine a friction term. The frozen saturated sand showed a higher ultimate strength than the frozen clay. This is due to the fact that the frozen clay usually contains a larger quantity of unfrozen water than the frozen saturated sand, at the same temperature. The confining pressure had no significant effect on the ultimate strength of the frozen clay (degree of saturation ≃ 96%); this is shown in Figure 5-9. This is similar to the behavior of unfrozen saturated clay under a similar stress history. The ultimate strength of the frozen saturated sand did increase with the increase in confining pressure, therefore implying the existence of a friction term in addition to the cohesion term in the sand-ice system. This is shown in Figure 5-10, with an angle of internal friction $\phi = 25°$.

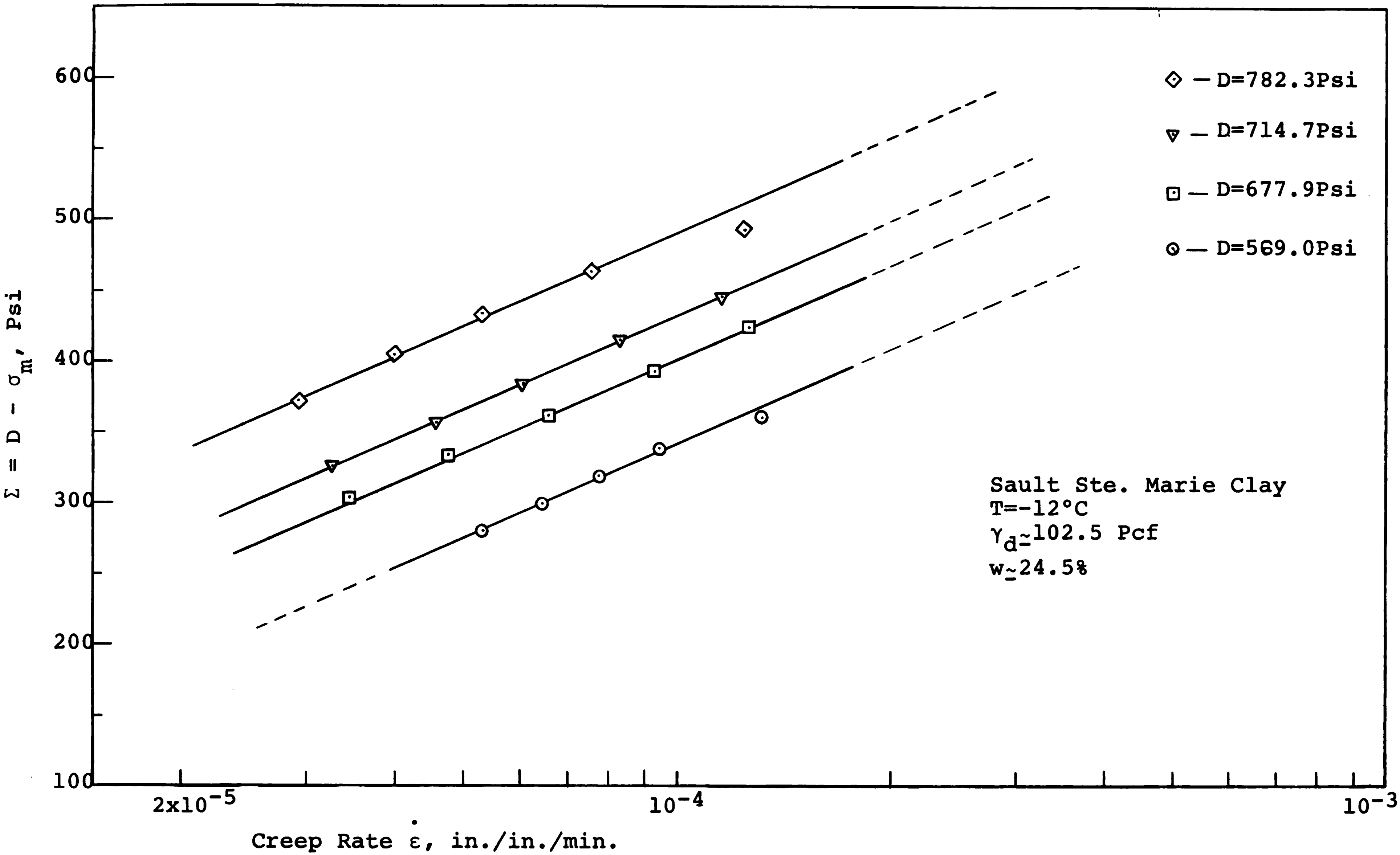

Figure 6-1. Creep Rate Versus Stress for Sault Ste. Marie Clay.

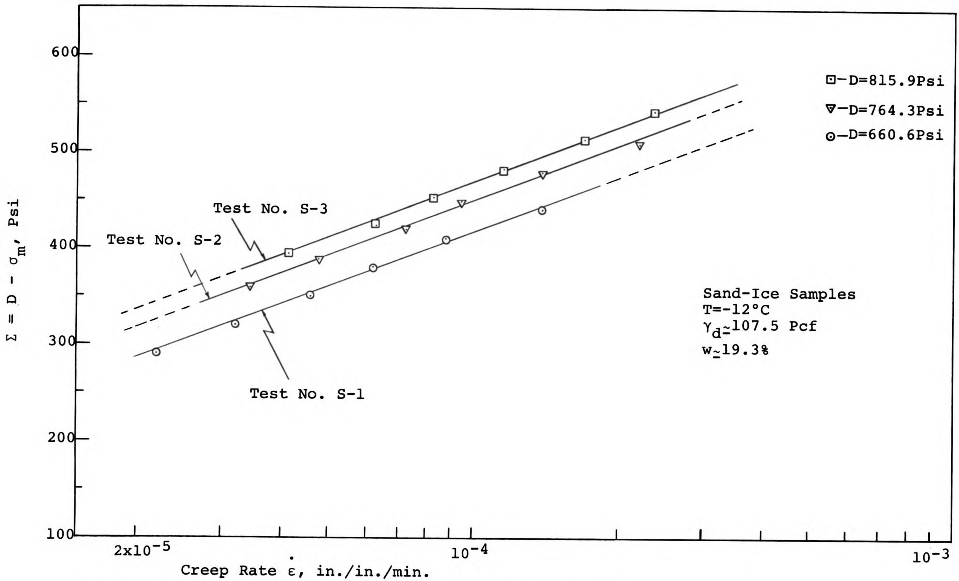

Figure 6-2. Creep Rate Versus Stress for Sand-Ice Samples.

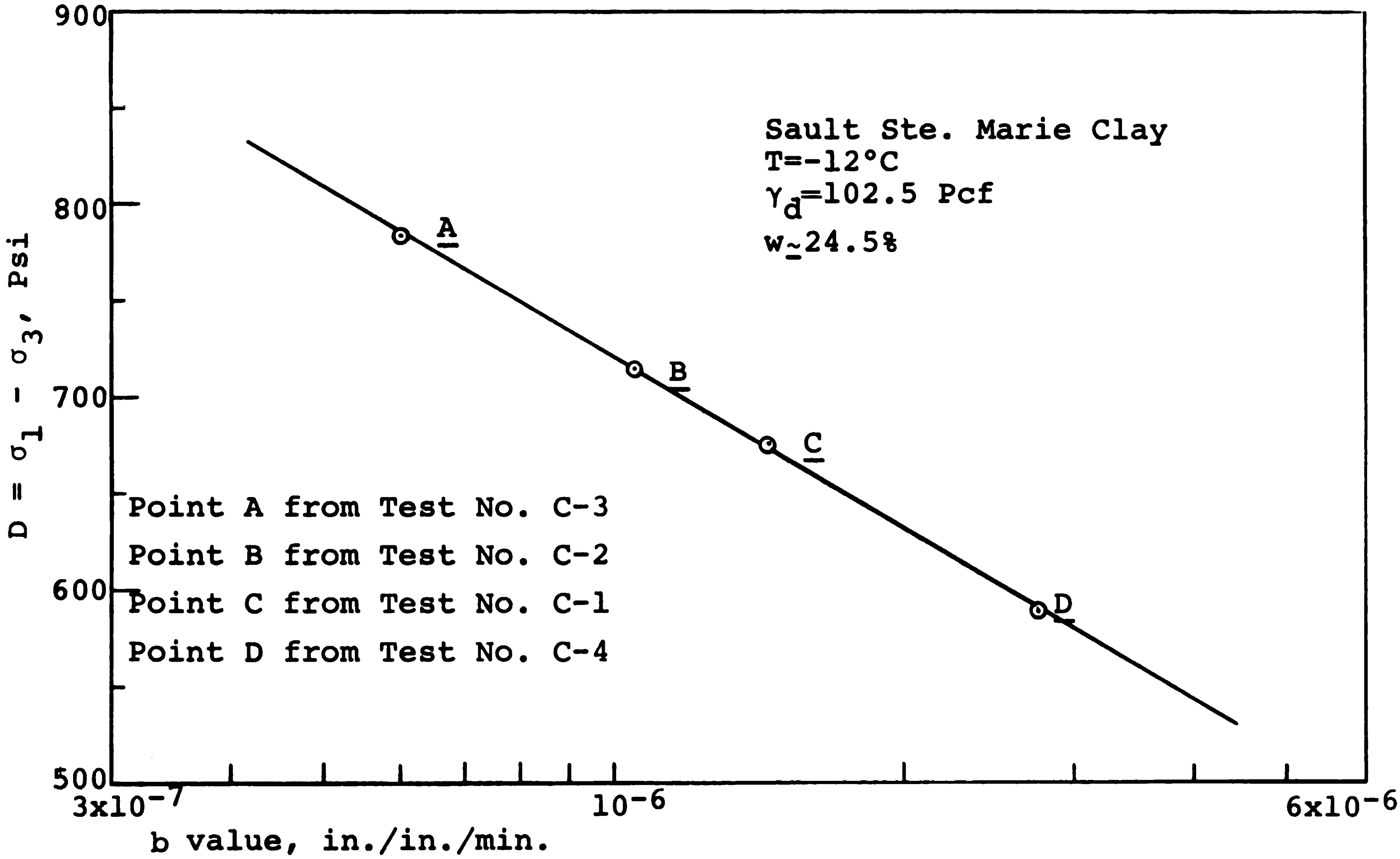

Figure 6-3. b Value Versus Stress Difference for Sault Ste. Marie.

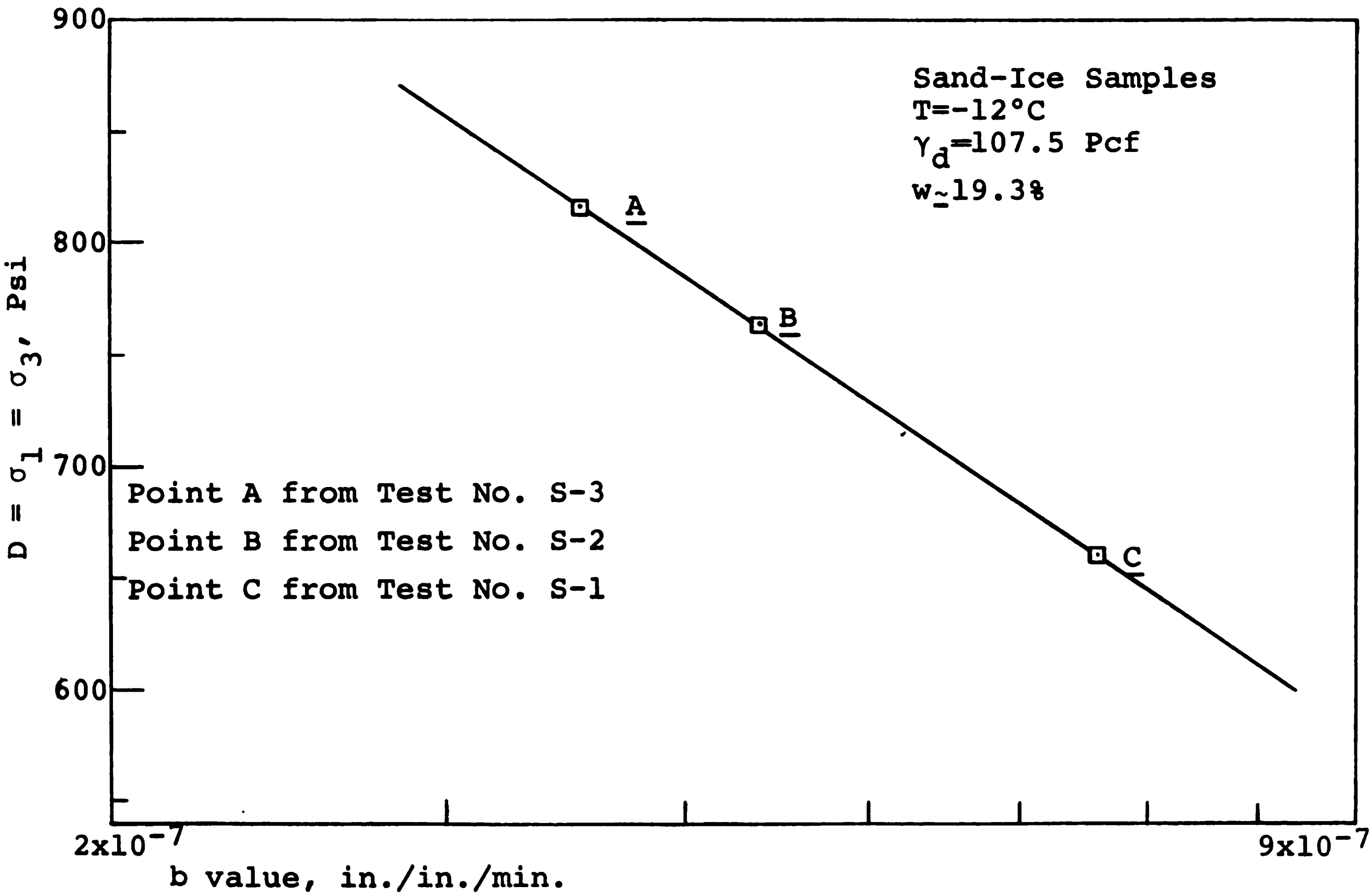

Figure 6-4. b Value Versus Stress Difference for Sand-Ice Samples.

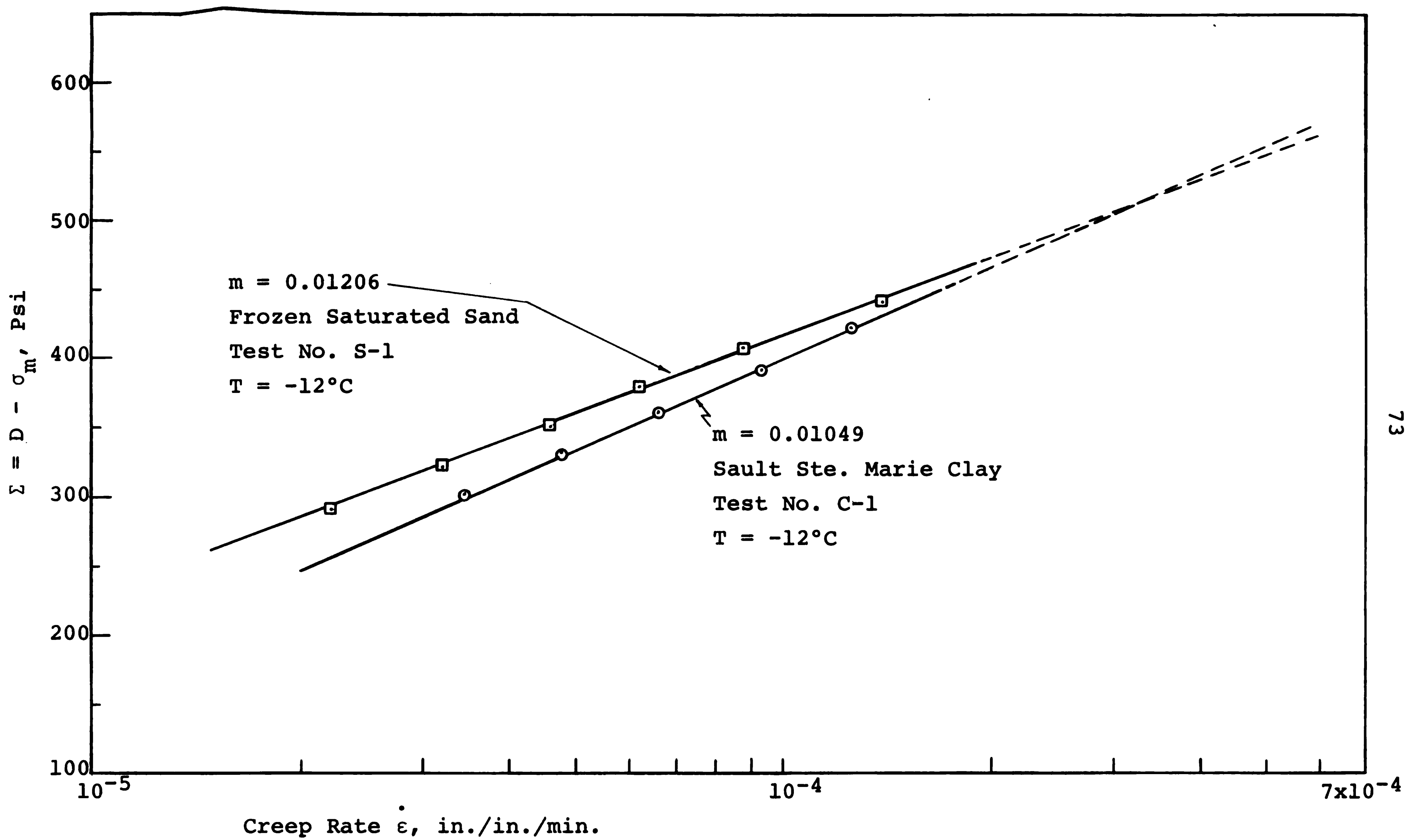

Figure 6-5. Typical Creep Rates Stress Curves for Sand-Ice Samples Compared With Sault Ste. Marie Clay Samples.

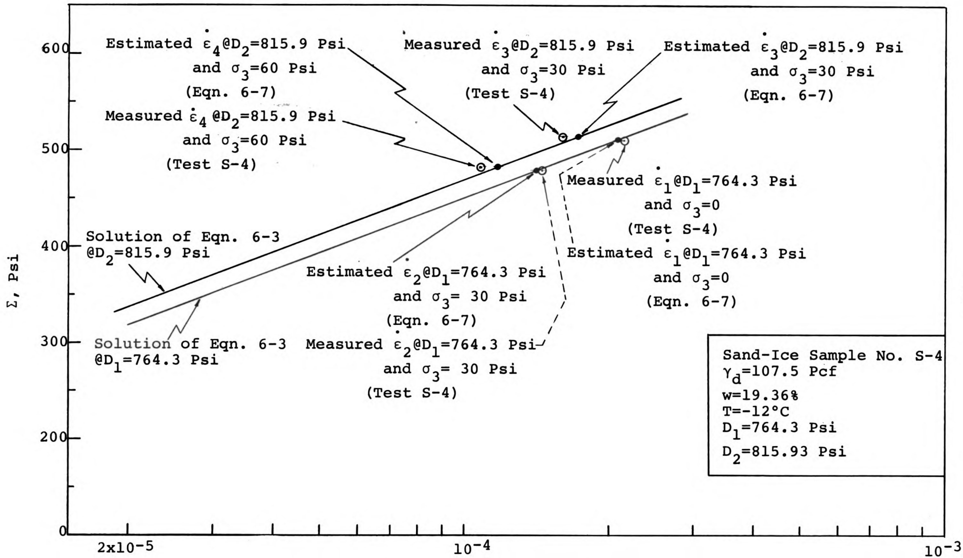

Figure 6-6. Measured and Estimated Creep Rates for Sand-Ice Material.

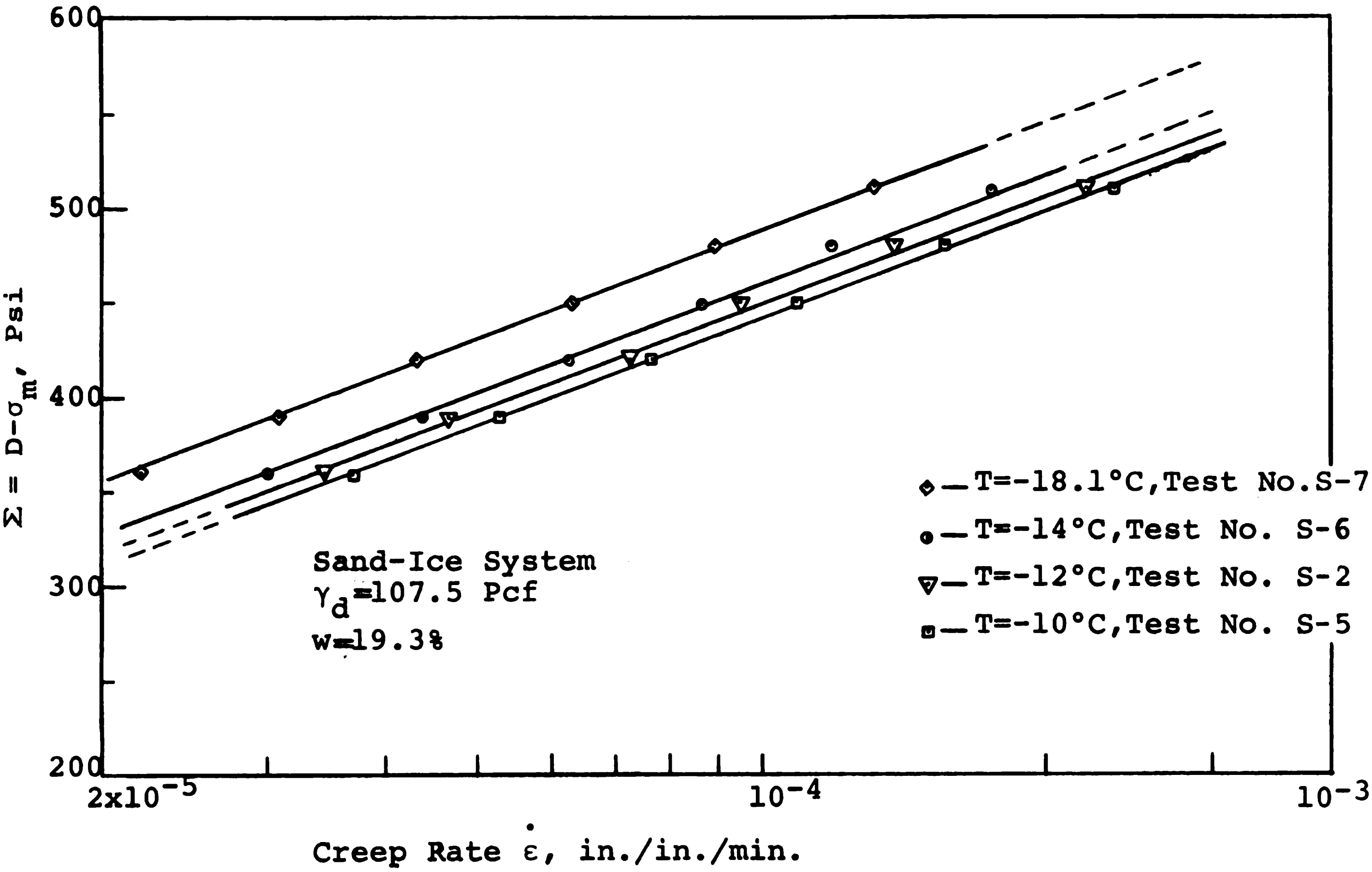

Figure 6-7. Dependence of Creep Rate on Stress and Temperature of Saturated Frozen Sand.

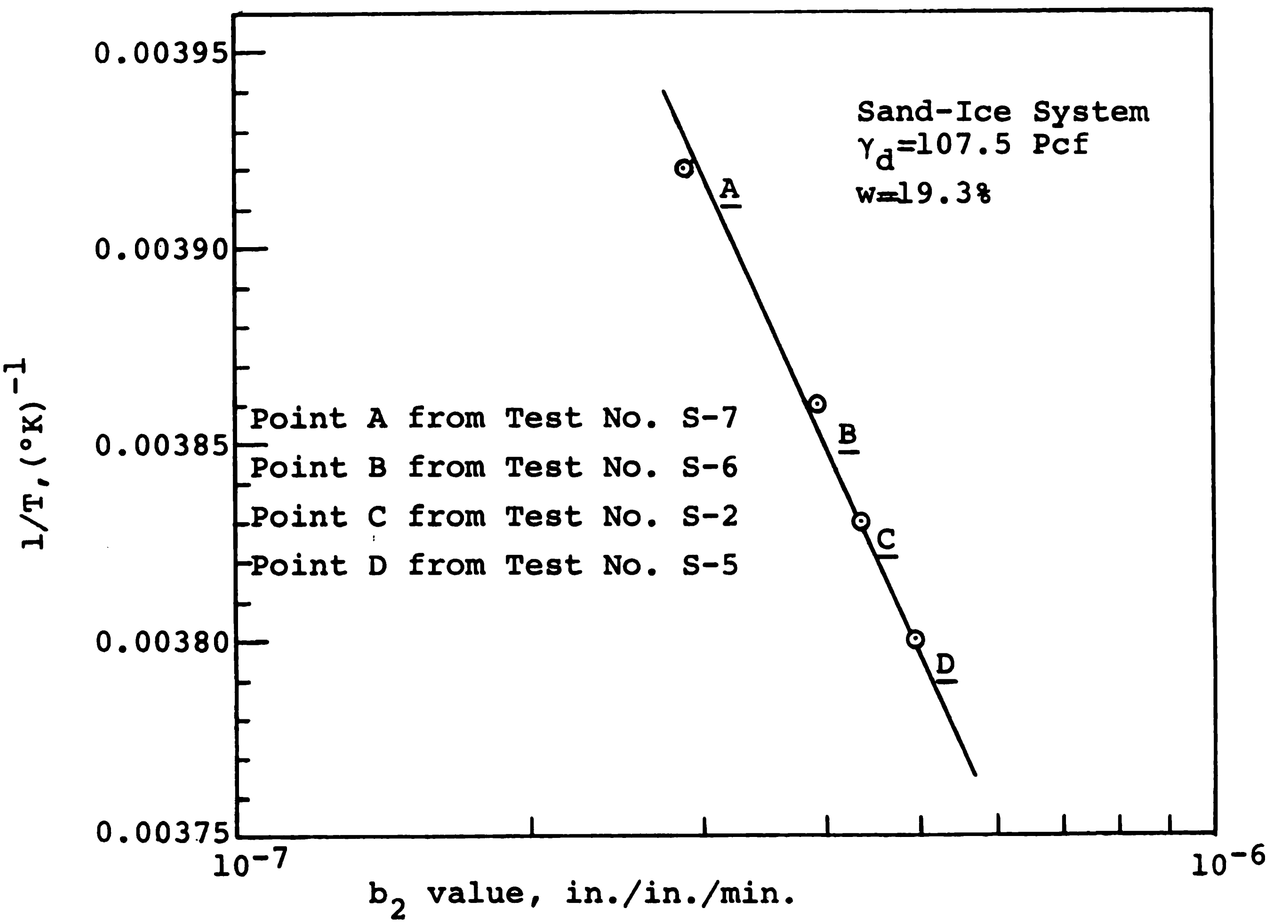

Figure 6-8. Temperature Dependence of b_2 in Equation (6-10).

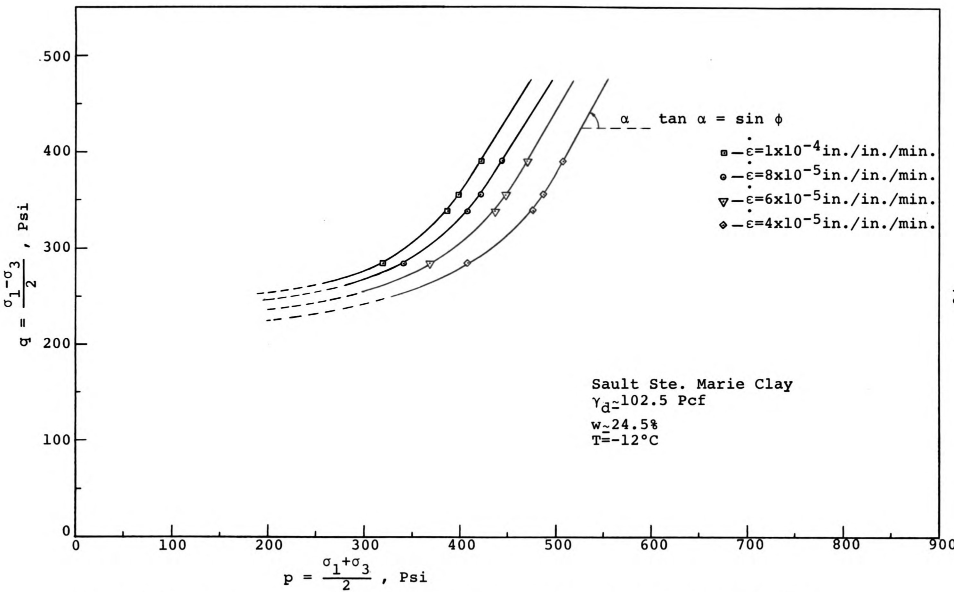

Figure 6-9. Time-Dependent Strength Behavior of Frozen Sault Ste. Marie Clay.

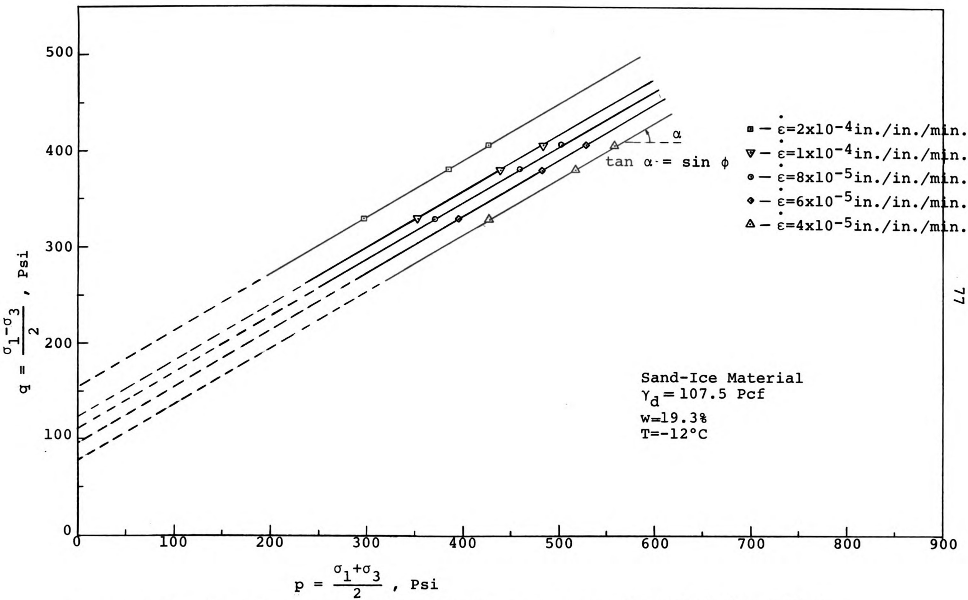

Figure 6-10. Time-Dependent Strength Behavior of Frozen Saturated Ottawa Sand.

CHAPTER VII

SUMMARY OF CONCLUSIONS

1. The results of the differential creep tests conducted in this study, on frozen Sault Ste. Marie clay and frozen saturated Ottawa sand, indicate that the mean stress does affect the creep rate of frozen soils. Therefore, the creep rate of frozen soil at a constant temperature must be considered as a function of the mean stress as well as the deviatoric stress. The creep rate increases exponentially with the increase in stress difference D, and decreases exponentially with the increase in mean stress σ_m. The steady state creep rate for frozen soils can be estimated, at a constant temperature, from the following equation:

$$\dot{\varepsilon} = C \cdot \exp\ (ND) \cdot \exp\ (-m\ \sigma_m)$$

where C, N, and m are parameters which can be determined by a differential creep test.

2. The effect of temperature on the creep behavior of frozen soils, under a constant stress difference, is described by an exponential function of the reciprocal of test temperature. This is in agreement with previous work showing that the creep phenomenon of frozen soil is a

thermally activated process. The effect of temperature on the creep rate can be described by the following equation:

$$\dot{\varepsilon} = C' \cdot \exp\ (-\ell/T) \cdot \exp\ (m\Sigma)$$

where $\Sigma = D-\sigma_m$, and C', ℓ, and m are parameters which can be evaluated from differential creep tests.

3. To combine the effect of both stress difference and test temperature on the steady state creep deformation of frozen soil, the experimental data suggest an equation of the following form:

$$\dot{\varepsilon} = A \cdot \exp\ (ND) \cdot \exp\ (-\ell/T) \cdot \exp\ (-m\ \sigma_m)$$

where A, N, ℓ, and m are parameters which can be evaluated experimentally. Tests were conducted so as to minimize changes in soil structure, which may influence some of the parameters. The equation above is in agreement with the general equation (Eqn. 6-14) describing creep deformation.

4. The time-dependent strength of frozen soil may be described by two parameters; a cohesion C and a friction angle ϕ, for a given creep rate. Results of differential creep tests, on frozen Sault Ste. Marie clay and frozen saturated sand, indicate that the friction angle ϕ appears to remain constant with change in creep rate, at constant temperature, while the cohesion C decreases with a slower creep rate, implying the dependence of C on time. Cohesion also depends on temperature. Values of C and ϕ can be

estimated, for a given creep rate, by using the equation describing the creep deformation.

5. The angle of friction ϕ for the sand-ice system can be considered independent of time and temperature; therefore it appears to be a property of the material. Cohesion is controlled by the properties of the ice matrix and any unfrozen water; thus it is time-dependent.

6. In a constant axial strain-rate compression test, at a relatively high strain-rate, the confining pressure has no significant effect on the ultimate strength of frozen clay, while the ultimate strength of frozen saturated sand does increase with the increase in confining pressure, therefore implying that friction does develop during deformation of saturated frozen sand. This would be in agreement with data reported by Goughnour (1967).

BIBLIOGRAPHY

BIBLIOGRAPHY

Andersland, O. B., and Akili, W. "Stress Effect on Creep Rates of a Frozen Clay Soil," Geotechnique, Vol. XVII, No. 1, March, 1967, pp. 27-39.

Bishop, A. W., and Henkel, D. J. The Measurement of Soil Properties in the Triaxial Test, Edward Arnold LTD, London, 1962.

Conrad, H. "Experimental Evaluation of Creep and Stress Rupture," Chapter 8, Mechanical Behavior of Materials at Elevated Temperature, Ed. by J. E. Dorn, McGraw-Hill Book Co., Inc., N. Y., 1961, p. 149.

Dillon, H. B., and Andersland, O. B. "Predicting Unfrozen Water Contents in Frozen Soils," Canadian Geotechnical J., Vol. III, No. 2., 1966, pp. 53-60.

Dillon, H. B., and Andersland, O. B. "Deformation Rates of Polycrystalline Ice," Int. Conf. on Physics of Snow and Ice, The Inst. of Low Temp. Sci., Hokkaido Univ., Sapporo, Japan, August, 1967.

Glasstone, S., Laidler, K. J., and Eyring, H. The Theory of Rate Processes, McGraw-Hill Book Co., Inc., N. Y., 1941.

Goughnour, R. R. "The Soil-Ice System and the Shear Strength of Frozen Soils," Ph.D. Thesis, Michigan State Univ., E. Lansing, Mich., 1967.

Goughnour, R. R., and Andersland, O. B. "Mechanical Properties of Sand-Ice System," Journal of the Soil Mechanics and Foundations Division, ASCE, Vol. 94 No. SM4, July, 1968.

Hill, R. "The Mathematical Theory of Plasticity." University Press, Oxford, 1950.

Lambe, T. W. "Stress Path Method," Journal of the Soil Mechanics and Foundations Division, ASCE, Vol. 93, No. SM6, November, 1967.

Leonards, G. A. "Strength Characteristics of Compacted Clays," Tans. ASCE, Vol. 120, 1955.

Leonards, G. A., and Andersland, O. B. "The Clay-Water System and the Shearing Resistance of Clays," ASCE Research Conf. on the Shear Strength of Cohesive Soils, Boulder, Colorado, 1960.

Mitchell, J. K., Campanella, R. G., and Singh, A. "Soil Creep as a Rate Process," Journal of the Soil Mechanics and Foundations Division, ASCE, Vol. 94, No. SM1, January, 1968.

Pounder, E. R. The Physics of Ice. Pergamon Press, Oxford, 1967.

Tsytovich, N. A. "Mechanical Properties of Frozen Soils." Chapter 4, Bases and Foundations on Frozen Soil, HRB Special Report 58, (A Translation from Russian), Washington, D. C., 1960.

Vialov, S. S. Ed., "The Strength and Creep of Frozen Soils and Calculations for Ice-Soil Retaining Structures," CRREL, Trans. 76, 1965a.

Vialov, S. S. Ed., "Investigation of the Cohesion of Frozen Soil," Chapter II, Rheological Properties and Bearing Capacity of Frozen Soils, CRREL, Trans. 74, September, 1965b.

Vialov, S. S. "Plasticity and Creep of a Cohesive Medium," Proc. of the Sixth Int. Conf. on Soil Mech. and Foundation Eng., Montreal, September, 1965c.

Appendix-Data

Table A-1.--Differential Creep Test Data

Test C-1.--Sault Ste. Marie Clay

$T = -12°C$

$\gamma_d = 102.2$ Pcf

$w = 24\%$

$L_o = 2.79$ in.

$d_o = 1.114$ in.

$D = 677.95$ Psi

Time (min.)	Deflection (in.)
@ $\sigma_3 = 0$	
0	0.00000
2	0.07329
4	0.08952
6	0.09351
8	0.09873
10	0.10190
12	0.10459
14	0.10691
16	0.10830
20	0.11056
25	0.11268
30	0.11498
34	0.11667
@ $\sigma_3 = 30$ Psi	
36	0.11781
38	0.11827
40	0.11893
42	0.11943
44	0.11995
46	0.12055
50	0.12157
55	0.12289
60	0.12426
64	0.12536

Time (min.)	Deflection (in.)
@ $\sigma_3 = 60$ Psi	
66	0.12656
68	0.12697
70	0.12748
72	0.12786
74	0.12809
76	0.12848
80	0.12925
85	0.13026
90	0.13133
94	0.13206
@ $\sigma_3 = 90$ Psi	
96	0.13324
98	0.13352
100	0.13388
102	0.13418
104	0.13434
106	0.13470
110	0.13518
115	0.13589
120	0.13659
124	0.13719
@ $\sigma_3 = 120$ Psi	
126	0.13842
128	0.13855
130	0.13878
132	0.13901
134	0.13928
136	0.13937
140	0.13976
145	0.14033
150	0.14079
154	0.14124

Table A-1.--Continued

Test C-1.--Continued

Time (min.)	Deflection (in.)
@ σ_3 = 150 Psi	
156	0.14234
158	0.14243
160	0.14254
162	0.14268
164	0.14284
166	0.14293
170	0.14325
175	0.14352
180	0.14391
184	0.14428

Test C-2.--Sault Ste. Marie Clay

$T = -12°C$

$\gamma_d = 101.7$ Pcf

$w = 24.30\%$

$L_o = 2.268$ in.

$d_o = 1.126$ in.

$D = 714.67$ Psi

Time (min.)	Deflection (in.)
@ σ_3 = 0	
0	0.00000
1	0.08348
2	0.09358
4	0.10248
6	0.10838
8	0.11238
10	0.11558
12	0.11818
15	0.12128
18	0.12398
20	0.12548
25	0.12858
30	0.13138
32	0.13238
34	0.13328
@ σ_3 = 30 Psi	
36	0.13448
38	0.13508
40	0.13558
42	0.13628
45	0.13703
50	0.13833
55	0.13958
60	0.14058
64	0.14148
@ σ_3 = 60 Psi	
66	0.14243
68	0.14258
70	0.14298
72	0.14343
75	0.14412
80	0.14483
85	0.14583
90	0.14663
94	0.14718
@ σ_3 = 90 Psi	
96	0.14813
98	0.14838
100	0.14862
102	0.14893
105	0.14948
110	0.15013
115	0.15073
120	0.15148
124	0.15173

Table A-1.--Continued

Test C-2.--Continued

Time (min.)	Deflection (in.)
@ σ_3 = 120 Psi	
126	0.15318
128	0.15348
130	0.15358
132	0.15398
135	0.15438
140	0.15493
145	0.15548
150	0.15593
155	0.15618
@ σ_3 = 150 Psi	
157	0.15763
160	0.15793
162	0.15813
165	0.15838
170	0.15866
175	0.15918
180	0.15955
184	0.15960
@ σ_3 = 120 Psi	
186	0.15958
188	0.15958
190	0.15958
192	0.15958
194	0.15963
195	0.15973
197	0.15990
200	0.16025
205	0.16058
210	0.16093
214	0.16123
@ σ_3 = 90 Psi	
216	0.16121
218	0.16121
220	0.16123
222	0.16125
224	0.16125

Time (min.)	Deflection (in.)
226	0.16130
228	0.16148
230	0.16155
240	0.16236
244	0.16256
@ σ_3 = 60 Psi	
247	0.16260
250	0.16268
252	0.16270
254	0.16288
256	0.16330
258	0.16340
260	0.16353
265	0.16388
270	0.16433
274	0.16453
@ σ_3 = 30 Psi	
276	0.16459
278	0.16460
280	0.16483
282	0.16505
285	0.16539
290	0.16578
295	0.16618
300	0.16659
304	0.16689
@ σ_3 = 0	
306	0.16703
308	0.16713
310	0.16733
312	0.16749
315	0.16780
320	0.16838
325	0.16863
330	0.16914
334	0.16948

Table A-1.--Continued

Test C-3.--Sault Ste. Marie Clay

T = -12°C

γ_d = 102.9 Pcf

w = 24.33%

L_o = 2.291 in.

d_o = 1.116 in.

D = 782.25 Psi

Time (min.)	Deflection (in.)
@ σ_3 = 0	
0	0.00000
1	0.10930
2	0.12180
4	0.13480
6	0.14200
8	0.14770
10	0.15226
12	0.15551
14	0.15877
16	0.16120
18	0.16351
20	0.16548
24	0.16883
28	0.17085
@ σ_3 = 30 Psi	
31	0.17330
32	0.17378
34	0.17433
36	0.17515
38	0.17586
40	0.17659
42	0.17699
44	0.17749
46	0.17790
48	0.17855
50	0.17910
54	0.18030
58	0.18130
59	0.18155

Time (min.)	Deflection (in.)
@ σ_3 = 60 Psi	
61	0.18270
62	0.18290
65	0.18340
67	0.18380
70	0.18430
72	0.18465
74	0.18500
76	0.18530
84	0.18665
88	0.18710
89	0.18735
@ σ_3 = 90 Psi	
91	0.18805
92	0.18810
94	0.18825
96	0.18850
98	0.18870
100	0.18890
102	0.18915
104	0.18945
106	0.18970
108	0.18990
110	0.19010
114	0.19045
118	0.19080
119	0.19090
@ σ_3 = 120 Psi	
121	0.19210
122	0.19215
124	0.19230
126	0.19255
128	0.19270
130	0.19280
132	0.19300
136	0.19330
138	0.19350
140	0.19365
145	0.19400
148	0.19406
149	0.19412

Table A-1.--Continued

Test C-3.--Continued

Time (min.)	Deflection (in.)
@ σ_3 = 150 Psi	
151	0.19556
152	0.19560
154	0.19575
156	0.19580
158	0.19590
160	0.19600
162	0.19630
164	0.19635
166	0.19648
168	0.19655
170	0.19670
174	0.19690
178	0.19695
179	0.19695
@ σ_3 = 120 Psi	
181	0.19695
182	0.19695
184	0.19695
186	0.19695
188	0.19698
190	0.19698
192	0.19700
194	0.19704
196.5	0.19710
198	0.19720
200	0.19735
204	0.19765
208	0.19780
209	0.19782
@ σ_3 = 90 Psi	
211	0.19772
212	0.19772
214	0.19772
216	0.19772
218	0.19772
222	0.19772
224	0.19774
227	0.19780
228	0.19782

Time (min.)	Deflection (in.)
230	0.19795
232	0.19800
234	0.19805
239	0.19832
@ σ_3 = 60 Psi	
241	0.19832
242	0.19832
244	0.19832
246	0.19832
248	0.19832
250	0.19832
252	0.19845
254	0.19860
256	0.19870
258	0.19885
260	0.19895
264	0.19924
268	0.19955
269	0.19960
@ σ_3 = 30 Psi	
271	0.19968
272	0.19968
274	0.19968
276	0.19968
278	0.19980
280	0.19995
282	0.20010
284	0.20020
286	0.20035
288	0.20050
290	0.20060
294	0.20095
298	0.20110
299	0.20120
@ σ_3 = 0	
301	0.20125
302	0.20125
304	0.20135
306	0.20155
308	0.20175
310	0.20195

Table A-1.--Continued

Test C-3.--Continued

Time (min.)	Deflection (in.)
312	0.20205
318	0.20270
320	0.20280
326	0.20310
328	0.20345
330	0.20370
332	0.20385
334	0.20400

Test C-4.--Sault Ste. Marie Clay

T = -12°C

γ_d = 102.8 Pcf

w = 24.13%

L_o = 2.29 in.

d_o = 1.123 in.

D = 569 Psi

Time (min.)	Deflection (in.)
@ σ_3 = 0	
0	0.00000
2	0.06065
5	0.06965
10	0.07695
12	0.07895
15	0.08105
18	0.08335
20	0.08445
22	0.08555
24	0.08655
@ σ_3 = 20 Psi	
26	0.08800
28	0.08875
30	0.08945
32	0.09005
34	0.09065
36	0.09130
38	0.09180
40	0.09240
@ σ_3 = 40 Psi	
43	0.09370
44	0.09415
46	0.09445
48	0.09495
50	0.09535
52	0.09569
55	0.09625
58	0.09674
@ σ_3 = 60 Psi	
60	0.09780
62	0.09820
64	0.09840
66	0.09875
68	0.09895
69	0.09914
@ σ_3 = 80 Psi	
70	0.09937
72	0.09957
75	0.10080
76	0.10095
78	0.10125
80	0.10140
82	0.10190
84	0.10205
86	0.10213
@ σ_3 = 100 Psi	
88	0.10340
90	0.10375
95	0.10435
100	0.10480
102	0.10505

Table A-1.--Continued

Test S-1.--Sand-Ice

T = - 12°C

γ_d = 107.5 Pcf

w = 19.42%

Ice density (Bulk) = 0.915 gm/cm^3

L_o = 2.26 in.

d_o = 1.13 in.

D = 660.6 Psi

Time (min.)	Deflection (in.)
@ σ_3 = 0	
0	0.00000
1	0.02130
2	0.02280
4	0.02600
6	0.02710
8	0.02810
14	0.02960
18	0.03110
20	0.03140
25	0.03300
29	0.03410
@ σ_3 = 30 Psi	
31	0.03490
32	0.03510
34	0.03550
36	0.03590
38	0.03640
40	0.03675
45	0.03770
50	0.03860
56	0.03960
59	0.04020
@ σ_3 = 60 Psi	
61	0.04100
62	0.04120

Time (min.)	Deflection (in.)
64	0.04144
66	0.04170
68	0.04204
70	0.04230
75	0.04300
80	0.04360
85	0.04430
89	0.04500
@ σ_3 = 90 Psi	
91	0.04580
92	0.04610
94	0.04620
96	0.04640
98	0.04660
100	0.04680
105	0.04735
110	0.04785
115	0.04835
119	0.04930
@ σ_3 = 120 Psi	
121	0.05025
124	0.05130
128	0.05160
130	0.05190
135	0.05235
140	0.05275
145	0.05320
149	0.05410
@ σ_3 = 150 Psi	
151	0.05495
152	0.05500
154	0.05520
157	0.05540
160	0.05555
165	0.05600
170	0.05645
175	0.05675
180	0.05680

Table A-1.--Continued

Test S-2.--Sand-Ice

T = - 12°C

γ_d = 107.5 Pcf

w = 19.32%

Ice density (bulk) = 0.910 gm/cm^3

L_o = 2.26 in.

d_o = 1.13 in.

D = 764.26 Psi

Time (min.)	Deflection (in.)
@ σ_3 = 0	
0	0.00000
1	0.01550
2	0.01650
4	0.01870
6	0.02060
8	0.02220
10	0.02380
12	0.02520
14	0.02650
16	0.02770
18	0.02900
20	0.03010
26	0.03310
29	0.03440
@ σ_3 = 30 Psi	
31	0.03550
32	0.03585
34	0.03660
36	0.03745
38	0.03810
40	0.03880
45	0.04040
50	0.04190
55	0.04340
59	0.04450
@ σ_3 = 60 Psi	
61	0.04540
62	0.04550
64	0.04600
66	0.04640
68	0.04675
70	0.04730
75	0.04830
80	0.04925
85	0.05040
89	0.05115
@ σ_3 = 90 Psi	
91	0.05185
92	0.05200
94	0.05230
96	0.05255
98	0.05290
100	0.05320
105	0.05400
110	0.05460
115	0.05550
119	0.05630
@ σ_3 = 120 Psi	
121	0.05715
122	0.05725
124	0.05750
126	0.05765
128	0.05790
130	0.05816
135	0.05865
140	0.05915
145	0.05955
149	0.06010
@ σ_3 = 150 Psi	
151	0.06145
152	0.06150
154	0.06160
156	0.06180
161	0.06225
165	0.06246
170	0.06288
175	0.06332
179	0.06370

Table A-1.--Continued

Test S-3.--Sand-Ice

T = -12°C

γ_d = 107.5 Pcf

w = 19.26%

Ice Density (bulk) = 0.907 gm/cm^3

L_o = 2.26 in.

d_o = 1.13 in.

D = 815.93 Psi

Time (min.)	Deflection (in.)
@ σ_3 = 0	
0	0.00000
1	0.03950
2	0.04090
4	0.04310
6	0.04480
8	0.04640
10	0.04790
12	0.04830
14	0.05065
16	0.05195
20	0.05410
25	0.05665
29	0.05880
@ σ_3 = 30 Psi	
31	0.06000
32	0.06050
34	0.06140
36	0.06225
38	0.06315
40	0.06395
45	0.06595
50	0.06780
55	0.06955
59	0.07095
@ σ_3 = 60 Psi	
61	0.07220
62	0.07240

Time (min.)	Deflection (in.)
64	0.07315
66	0.07370
68	0.07425
70	0.07480
75	0.07616
80	0.07750
85	0.07870
89	0.07955
@ σ_3 = 90 Psi	
91	0.08105
92	0.08120
94	0.08175
96	0.08215
98	0.08250
100	0.08290
105	0.08385
110	0.08470
115	0.08555
119	0.08620
@ σ_3 = 120 Psi	
121	0.08780
122	0.08785
124	0.08820
126	0.08846
128	0.08870
130	0.08910
135	0.08975
140	0.09030
145	0.09106
149	0.09150
@ σ_3 = 150 Psi	
151	0.09315
152	0.09320
154	0.09325
156	0.09355
158	0.09380
160	0.09410
165	0.09450
170	0.09510
175	0.09560
179	0.09600

Table A-1.--Continued

Test S-4.--Sand-Ice

T = -12°C

γ_d = 107.5 Pcf

w = 19.36%

Ice density (bulk) = 0.912 gm/cm^3

L_o = 2.26 in.

d_o = 1.13 in.

D = 764.26 Psi, then 815.93 Psi

Time (min.)	Deflection (in.)
@ D = 764.26 Psi, σ_3 = 0	
0	0.00000
1	0.01940
2	0.02160
4	0.02480
6	0.02740
8	0.02970
10	0.03180
12	0.03350
15	0.03610
20	0.03965
25	0.04270
30	0.04540
34	0.04740
@ D = 764.26 Psi, σ_3 = 30 Psi	
36	0.04855
38	0.04945
40	0.05025
42	0.05100
45	0.05215
50	0.05375
55	0.05530
60	0.05665
64	0.05760

Time	Deflection
@ D = 815.93 Psi, σ_3 = 30 Psi	
66	0.05930
68	0.05995
70	0.06065
72	0.06141
76	0.06277
80	0.06396
85	0.06566
90	0.06740
94	0.06866
@ D = 815.93 Psi, σ_3 = 60 Psi	
96	0.06959
98	0.07004
100	0.07052
105	0.07171
110	0.07291
115	0.07397
120	0.07515
125	0.07621

Test S-5.--Sand-Ice

T = -10°C

γ_d = 107.5 Pcf

w = 19.37%

Ice density (bulk) = 0.913 gm/cm^3

L_o = 2.26 in.

d_o = 1.13 in.

D = 764.26 Psi

Table A-1.--Continued

Test S-5.--Continued

Time (min.)	Deflection (in.)
@ σ_3 = 0	
0	0.00000
1	0.01120
2	0.01280
4	0.01550
6	0.01790
8	0.02010
10	0.02220
12	0.02445
15	0.02690
21	0.03140
25	0.03390
30	0.03670
34	0.03855
@ σ_3 = 30 Psi	
36	0.04040
38	0.04110
40	0.04190
42	0.04255
45	0.04375
50	0.04545
55	0.04700
60	0.04850
64	0.05015
@ σ_3 = 60 Psi	
66	0.05160
68	0.05195
70	0.05250
72	0.05285
75	0.05366
80	0.05470
85	0.05580
90	0.05675
94	0.05765

Time (min.)	Deflection (in.)
@ σ_3 = 90 Psi	
96	0.05935
98	0.05955
100	0.05985
102	0.06020
105	0.06065
110	0.06140
115	0.06210
120	0.06290
124	0.06375
@ σ_3 = 120 Psi	
126	0.06518
128	0.06550
130	0.06570
133	0.06600
135	0.06625
140	0.06675
145	0.06720
150	0.06775
154	0.06825
@ σ_3 = 150 Psi	
156	0.06960
158	0.06980
160	0.06995
162	0.07010
165	0.07035
170	0.07880
175	0.07115
180	0.07155
185	0.07190

Table A-1.--Continued

Test S-6.--Sand-Ice

T = -14°C

γ_d = 107.5 Pcf

w = 19.34%

Ice density (bulk) = 0.911 gm/cm^3

L_o = 2.26 in.

d_o = 1.13 in.

D = 764.26 Psi

Time (min.)	Deflection (in.)
@ σ_3 = 0	
0	0.00000
1	0.01350
2	0.01460
4	0.01660
6	0.01830
8	0.01960
10	0.02090
12	0.02210
15	0.02360
20	0.02610
25	0.02810
30	0.03000
34	0.03150
@ σ_3 = 30 Psi	
36	0.03250
38	0.03310
40	0.03365
42	0.03420
45	0.03505
50	0.03655
55	0.03760
60	0.03885
64	0.04000

Time (min.)	Deflection (in.)
@ σ_3 = 60 Psi	
66	0.04080
68	0.04125
70	0.04160
72	0.04210
75	0.04265
80	0.04360
85	0.04450
90	0.04535
94	0.04625
@ σ_3 = 90 Psi	
96	0.04700
98	0.04730
100	0.04760
102	0.04785
105	0.04825
110	0.04890
115	0.04960
120	0.05030
124	0.05115
@ σ_3 = 120 Psi	
126	0.05220
128	0.05245
130	0.05260
135	0.05310
140	0.05360
145	0.05410
150	0.05465
154	0.05560
@ σ_3 = 150 Psi	
156	0.05650
158	0.05665
160	0.05680
165	0.05715
170	0.05750
175	0.05780
180	0.05825
185	0.05860

Table A-1.--Continued

Test S-7.--Sand-Ice

T = -18.1°C

γ_d = 107.5 Pcf

w = 19.40%

Ice density (bulk) = 0.914 gm/cm^3

L_o = 2.26 in.

d_o = 1.13 in.

D = 764.26 Psi

Time (min.)	Deflection (in.)
@ σ_3 = 0	
0	0.00000
1	0.01290
2	0.01295
4	0.01315
6	0.01408
8	0.01479
10	0.01535
12	0.01585
15	0.01665
20	0.01815
25	0.01955
30	0.02075
34	0.02170
@ σ_3 = 30 Psi	
36	0.02320
38	0.02330
40	0.02365
45	0.02460
50	0.02555
55	0.02635
60	0.02720
64	0.02807
@ σ_3 = 60 Psi	
66	0.03002
68	0.03020

Time (min.)	Deflection (in.)
70	0.03045
75	0.03124
80	0.03196
85	0.03262
90	0.03339
94	0.03406
@ σ_3 = 90 Psi	
96	0.03545
100	0.03565
105	0.03620
110	0.03670
115	0.03725
120	0.03765
124	0.03815
@ σ_3 = 120 Psi	
126	0.03950
128	0.03965
130	0.03975
135	0.04018
140	0.04060
145	0.04100
150	0.04140
154	0.04162
@ σ_3 = 150 Psi	
156	0.04330
158	0.04335
160	0.04342
162	0.04355
165	0.04366
170	0.04395
175	0.04425
180	0.04455
185	0.04485

Table A-2.--Constant Strain-Rate Test Data

Test CF-1.--Sault Ste. Marie Clay

$T = -12°C$

$\gamma_d = 103.1$ Pcf.

$w = 24.61\%$

$L_o = 2.26$ in.

(1) $A_o = 0.98134$ in.^{2}

$\dot{\varepsilon} = 3 \times 10^{-3}$ in./in./min.

$\sigma_3 = 30$ Psi

Time (min.)	Deflection (in.)	Load (lbs.)
1	0.00500	182.4
2	0.01790	396.6
4	0.03800	519.7
6	0.05400	574.5
8	0.06650	601.8
10	0.07775	629.2
12	0.08870	651.9
14	0.10115	683.9
16	0.11560	711.2
18	0.12880	729.5
20	0.14170	756.8
22	0.15490	775.1
24	0.16675	788.7
26	0.17850	802.4
28	0.19020	820.6
30	0.20245	834.3
32	0.21480	848.0
34	0.22660	861.7
36	0.23890	875.4
38	0.25080	884.5
40	0.26270	893.6

Test CF-2.--Sault Ste. Marie Clay

$T = -12°C$

$\gamma_d = 102.6$ Pcf

$w = 24.49\%$

$L_o = 2.26$ in.

$A_o = 0.95390$ in.^{2}

$\dot{\varepsilon} = 3 \times 10^{-3}$ in./in./min.

$\sigma_3 = 60$ Psi

Time (min.)	Deflection (in.)	Load (lbs.)
1	0.00630	159.6
2	0.01415	332.8
4	0.03210	483.3
6	0.04580	547.1
8	0.06050	592.7
10	0.07515	624.6
12	0.08750	647.4
14	0.10000	674.7
16	0.11230	697.5
18	0.12510	720.4
20	0.13870	743.2
22	0.15175	755.7
24	0.16500	773.9
26	0.17850	791.0
28	0.19200	800.8
30	0.20575	817.9
32	0.21850	832.2
34	0.23050	842.5
36	0.24265	854.1
38	0.25490	862.9
40	0.26700	871.4

---

(1) The corrected sample area, $A = \frac{A_0}{1-\varepsilon}$

Table A-2.--Continued

Test CF-3.--Sault Ste. Marie Clay

$T = -12°C$

$\gamma_d = 102.5$ Pcf

$w = 24.23\%$

$L_o = 2.26$ in.

$A_o = 0.98134$ in.^{2}

$\dot{\varepsilon} = 3 \times 10^{-3}$ in./in./min.

$\sigma_3 = 90$ Psi

Time (min.)	Deflection (in.)	Load (lbs.)
1	0.00530	118.5
2	0.01250	319.1
4	0.03150	510.6
6	0.04650	574.5
8	0.06035	610.9
10	0.07415	647.4
12	0.08800	674.8
14	0.10150	702.1
16	0.11565	724.9
18	0.12950	747.7
20	0.14350	765.9
22	0.15765	784.2
24	0.17175	802.4
26	0.18575	820.6
28	0.19900	834.3
30	0.21195	848.0
32	0.22475	861.7
34	0.23805	875.4
36	0.25075	884.5
38	0.26350	898.2
40	0.29275	907.3
42	0.31925	916.4

Test SF-1.--Sand-Ice

$T = -12°C$

$\gamma_d = 107.5$ Pcf

$w = 19.40\%$

Ice density (bulk) = 0.914 gm/cm^3

$L_o = 2.26$ in.

$A_o = 1$ in.^{2}

$\dot{\varepsilon} = 3 \times 10^{-3}$ in./in./min.

$\sigma_3 = 30$ Psi

Time (min.)	Deflection (in.)	Load (lbs.)
0.5	0.00450	24.7
1.0	0.00690	78.5
1.5	0.00999	224.4
2.0	0.01250	390.4
2.5	0.01585	642.1
3.0	0.01921	865.6
3.5	0.02297	1071.3
4.0	0.02624	1200.1
4.5	0.03081	1320.2
5.0	0.03508	1393.3
5.5	0.03867	1422.8
6.0	0.04200	1428.6
6.5	0.04539	1437.3
7.0	0.04855	1444.0
7.5	0.05131	1418.6
8.0	0.05402	1414.9
8.5	0.05630	1407.6
9.0	0.05854	1404.2
9.5	0.06130	1398.5
10.0	0.06405	1398.7
10.5	0.06769	1399.9
11.0	0.07113	1396.4
11.5	0.07411	1395.2
12.0	0.07714	1400.2
12.5	0.08046	1397.9
13.0	0.08362	1397.7

Table A-2.--Continued

Test SF-3.--Sand-Ice

$T = -12°C$

$\gamma_d = 107.5$ Pcf

$w = 19.35\%$

Ice density (bulk) = 0.912 gm/cm^3

$L_o = 2.26$ in.

$A_o = 1$ in.^{2}

$\dot{\varepsilon} = 3 \times 10^{-3}$ in./in./min.

$\sigma_3 = 60$ Psi

Time (min.)	Deflection (in.)	Load (lbs.)
0.5	0.00412	38.2
1.0	0.00624	105.6
1.5	0.00963	220.4
2.0	0.01219	353.6
2.5	0.01625	586.8
3.0	0.01978	826.2
3.5	0.02324	1017.1
4.0	0.02525	1130.1
4.5	0.02972	1300.3
5.0	0.03542	1434.2
5.5	0.03838	1470.0
6.0	0.04091	1483.1
6.5	0.04419	1487.9
7.0	0.04688	1469.9
7.5	0.04988	1449.2
8.0	0.05246	1433.1
8.5	0.05707	1422.2
9.0	0.06066	1420.5
9.5	0.06471	1428.1
10.0	0.06848	1439.2
10.5	0.07183	1448.6
11.0	0.07479	1454.3
11.5	0.07877	1454.3
12.0	0.08200	1453.9
12.5	0.08744	1449.8
13.0	0.09226	1441.2

Test SF-3.--Sand-Ice

$T = -12°C$

$\gamma_d = 107.5$ Pcf

$w = 19.42\%$

Ice density (bulk) = 0.915 gm/cm^3

$L_o = 2.26$ in.

$A_o = 1$ in.^{2}

$\dot{\varepsilon} = 3 \times 10^{-3}$ in./in./min.

$\sigma_3 = 90$ Psi

Time (min.)	Deflection (in.)	Load (lbs.)
0.5	0.00624	42.6
1.0	0.00742	79.4
1.5	0.01060	210.6
2.0	0.01334	330.5
2.5	0.01558	466.2
3.0	0.01831	619.1
3.5	0.02166	879.7
4.0	0.02532	1137.9
4.5	0.02900	1300.7
5.0	0.03311	1426.5
5.5	0.03831	1503.8
6.0	0.04360	1533.9
6.5	0.04624	1532.4
7.0	0.04814	1521.9
7.5	0.05131	1497.3
8.0	0.05368	1467.0
8.5	0.05797	1433.0
9.0	0.06143	1418.9
9.5	0.06466	1404.9
10.0	0.06769	1400.4
10.5	0.07140	1395.2
11.0	0.07499	1395.0
11.5	0.07881	1401.0
12.0	0.08270	1410.6
12.5	0.08733	1415.1
13.0	0.09163	1420.7